NPL Report MATC (A) 95

Steam Turbine Operating Conditions, Chemistry of Condensates, and Environment Assisted Cracking – A Critical Review

Shengqi Zhou and Alan Turnbull

May 2002

Date: May 2002

Steam Turbine Operating Conditions, Chemistry of Condensates, and Environment Assisted Cracking – A Critical Review

Shengqi Zhou and Alan Turnbull
Materials Centre
National Physical Laboratory
Teddington, Middlesex, UK, TW11 0LW

ABSTRACT

A review of the literature and discussions with plant operators has been undertaken to establish present knowledge and understanding of the chemistry of the condensates formed on steam turbines and the link to system operation. This has been supplemented by an overview of the effect of test variables on environment assisted cracking.

In Section 1, steam turbine operating conditions are described including the steam cycle, the chemical control of the steam/water circuit and the distribution of temperature, pressure and steam wetness in the turbine. Service experience indicates that cracking occurs mainly in regions where condensates form. The saturation temperature, at which condensation occurs, varies from station to station, depending on the turbine design and operating conditions. Calculations based on thermodynamic data under steady flow conditions show that the concentration of non-volatile species (e.g. chloride, sulphate, sodium, etc.) in the liquid phase can be 100 times higher than that in the steam. Much higher concentrations of these species may be present in deposits in the regions where the steam is dry or dry/wet cycles occur. On the other hand, the concentration of volatile species (e.g. oxygen, carbon dioxide) in the liquid phase is usually less than 1 ppb under normal operating conditions. However, concentrations of oxygen and carbon dioxide in the condensates can be as high as several ppm under transient conditions (forced condensation, air leakage, off-load and start-up).

In Section 2, stress corrosion cracking (SCC) data for disc steels are reviewed critically. The effect of material properties (steel cleanliness, yield strength), environment (oxygen, carbon dioxide, chloride level), temperature, and stress conditions, on the initiation and growth of stress corrosion cracks is assessed. For long cracks, growth rates are claimed to be independent of oxygen and CO_2 concentration, and steel cleanliness, but there are some exceptions that suggest that the apparent independence of these variables may be linked partly to the spread in growth rate data. Unquestionably, the variables having the most dramatic effect are strength level and temperature. Dissolved gases and steel cleanliness have a more profound influence on "initiation" of stress corrosion cracks for medium strength disc steels, certainly in relation to pit development and growth but the impact on short crack growth is less well established.

Keywords: **Steam turbine, water/steam chemistry, stress corrosion cracking, environment assisted cracking**

ISSN 1473-2734

National Physical Laboratory
Teddington, Middlesex, UK, TW11 0LW

Approved on behalf of Managing Director, NPL, by Dr C Lea,
Head, Materials Centre

CONTENTS

INTRODUCTION

The power industry has experienced failures from environment assisted cracking (EAC) of steam turbine blades, discs and rotors. Despite worldwide effort, occasional problems still arise. The major challenge is to predict more reliably the conditions under which cracking is likely and, for those conditions, the evolution of crack size with time so that non-destructive testing may be used in a focused manner and informed decisions made about inspection intervals and remnant life. The difficulty is the complexity and transient nature of service conditions, and constraints in their detailed characterisation, e.g. the chemistry of the condensate formed on the turbine steel surface.

Stress corrosion cracking (SCC) of steam turbine disc and blade steels, especially for long cracks, has been studied for more than 30 years. However, the data generated can show inconsistency for often nominally the same conditions. This is in part due to a lack of control of test conditions. However, it is also the case that the scientific framework for interpretation of the data has not been adequate in many applications and apparently similar test conditions have subtle differences which are overlooked.

The objectives of this review are twofold: viz. to establish current knowledge and understanding of the link between steam chemistry and the chemistry of the condensate on the turbine steels, with particular emphasis on out-of-specification steam chemistry and on-load and off-load transients; to review critically existing literature on the effect of test variables on EAC.

SECTION 1 STEAM TURBINE OPERATING CONDITIONS

Introduction

It has long been established that many problems of steam turbine operation, e.g. erosion corrosion, pitting and environment assisted cracking (EAC), deposit build-up and the associated loss of efficiency, are related to the impurities in the steam. As a result, extensive studies on the water and steam chemistry have been conducted for many decades. In particular, EPRI[1-6] has organised a number of consecutive projects and produced several comprehensive reports on carry-over, partitioning and deposition of impurities in the steam.

The steam turbine operating conditions are complex and vary from station to station. It is not intended to conduct a review covering all aspects related to the operating conditions. Rather, the review will focus on the influence of impurities, such as chloride, oxygen and carbon dioxide on the solution composition of the condensate formed on the surface of discs and blades. The composition of deposits and the effect of crevices on the local chemistry will also be evaluated.

Steam Turbine Operating Conditions

The Steam cycle

The essential elements of the steam cycle include the boiler (or steam generator), turbines, generator and condenser. A simplified steam cycle[7], in this case with a drum-type boiler, is shown schematically in Figure 1.

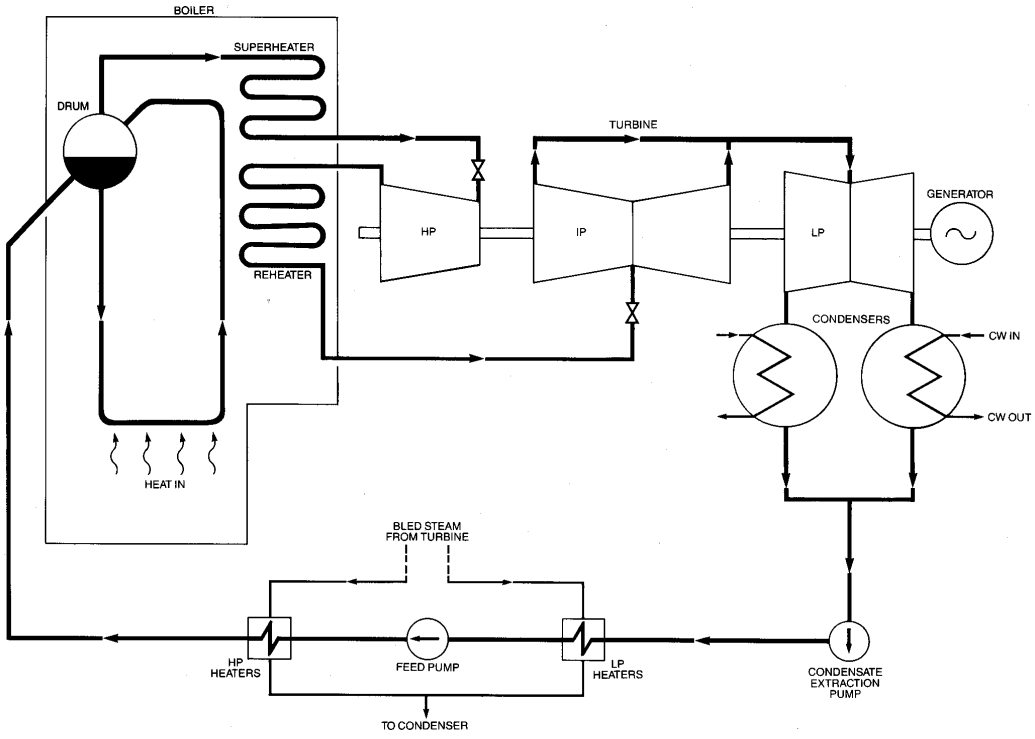

Figure 1. Simplified steam cycle in the power plant[7].

There are two types of steam/water circuit, i.e. the drum-type and once-through systems. The drum-type units operate at sub-critical pressures (i.e. below about 220 bar) with water separated from the saturated steam in the steam drum. The dry steam then passes to the superheater where the temperature is raised to the required level. The advantage of the drum type units compared with a once-through design (see below), as far as cycle chemistry is concerned, is that the steam-water separation stage in the steam drum of a sub-critical steam generator allows greater flexibility in terms of the additives that can be used for water treatment. For example, phosphate treatments can be used to convert residual concentrations of calcium and other "hardness" salts to their respective phosphate compounds. These compounds can be more readily dispersed and removed by blow-down (although there may be some carry over in high pressure units). The tendency of solid constituents to remain with the water phase makes this possible. Thus, a drum-type unit has the ability to operate with marginal feedwater quality.

The once-through unit operates above the critical pressure. Since the water does not boil in these so-called supercritical units, there is no need for a steam drum to separate the water and steam. Thus, a once-through unit operating at supercritical pressure consists (in simple terms) of a length of tubing through which water is pumped and to which heat is transferred. Within a certain enthalpy range (1980-2446 kJ/kg) the fluid undergoes a transition from a liquid to a vapour. The advantage of operating at the higher temperatures and pressures associated with a supercritical unit is that the efficiency of power generation is increased compared with units operating at sub-critical conditions.

Since water is converted completely to steam in a once-through unit, solids in the feedwater must ultimately deposit in the boiler, the superheater, or the turbine. Although high-quality make-up water can be provided consistently, the condenser always represents a possible source of contamination. Thus, demineralisation of the condensate is necessary in systems with once-through boilers if operation is not to be curtailed during condenser leaks. In practical terms, only all-volatile treatments (eg. ammonia or hydrazine) can be used in once-through units and recently oxygen treatments have become popular, with oxygen levels being controlled in the 25 ppb - 50 ppb range. In principle, the oxygenated treatment commonly used in once-through units could also be applied to a drum-type units provided other impurities are maintained at a very low level by condensate polishing.

Clearly, the differences between the cycle chemistry in the once-through and drum-type units will have implications for the environment in the power train down-stream of the steam generator.

The turbines

Examples of HP, IP and LP turbines[8,9] are shown in Figures 2 and 3. The major components are rotors, discs, blades, valves and bolts.

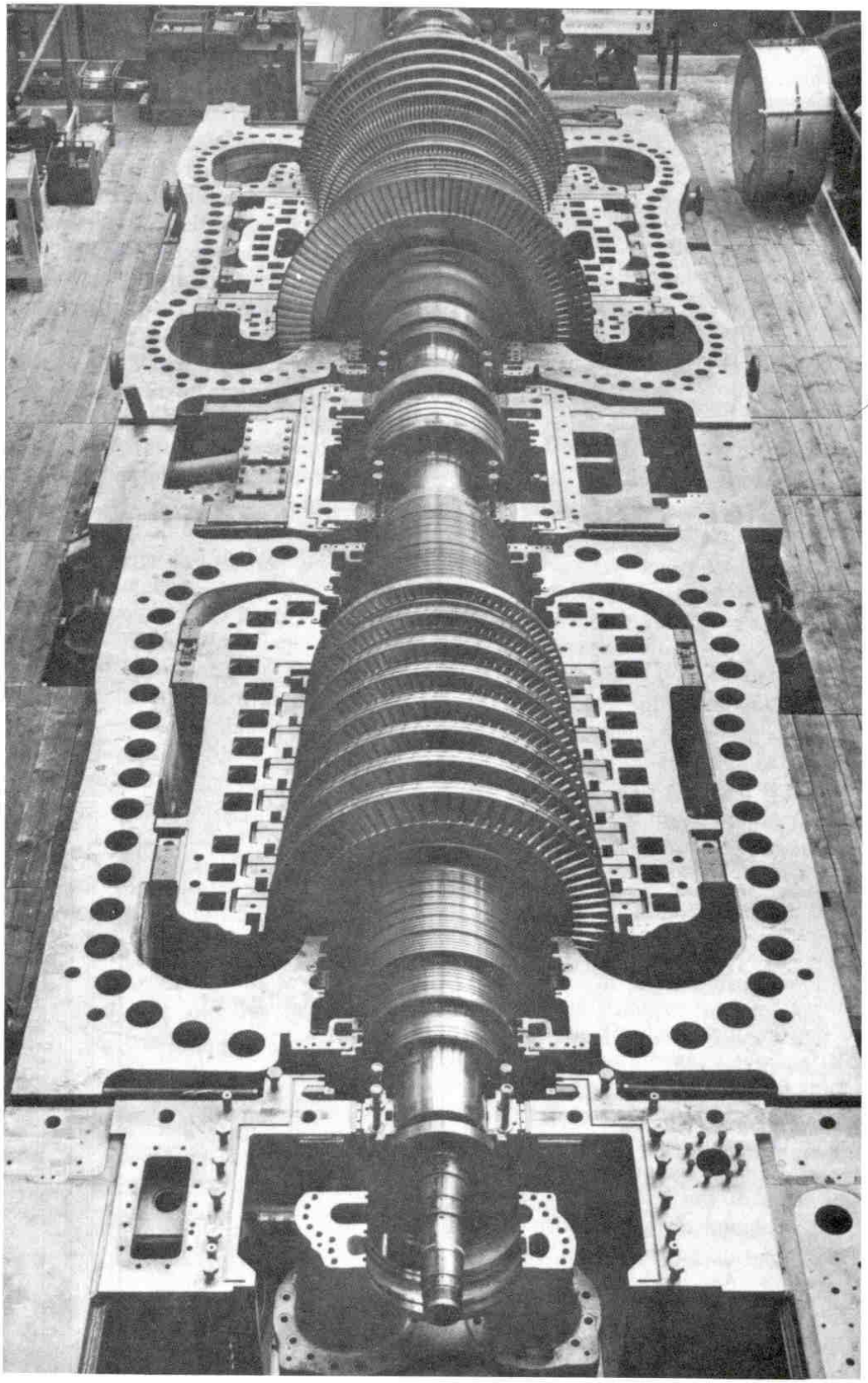

Figure 2. High and intermediate pressure steam turbines[8].

Figure 3. Low pressure steam turbines[9].

Chemistry control of the steam/water circuit

In power plants, the boiler and feed-water is pre-treated and controlled to minimise the risk of corrosion damage and deposition problems in the boiler, tubing, superheater, reheater and turbines, and loss of efficiency or output. Figure 4 is a schematic diagram showing the locations of principal monitoring and dosing points for an Advanced Gas-cooled Reactor (AGR) once-through unit. It should be noted that the location of sampling and dosing points depends on the design of power plant and the type of steam generator. Therefore, Figure 4 should be considered for illustration purposes only.

The guidelines for chemical control of boiler and feed-water and steam have been set nationally[10] and internationally[11-14] and the main control target is the cation conductivity. Other aggressive impurities, e.g. chloride and sulphate, are also recommended to be monitored separately.

Cation conductivity

The cation conductivity, also termed *conductivity after cation exchange* or *acid conductivity*, is the conductivity measured in a sample which has been passed through a column of strong cation exchange resin. The column substitutes H^+ for the cations so that the resulting solution contains the acids of the contaminating anions. The cation conductivity is a reliable indicator of the presence of contamination from inorganic species such as chlorides, sulphates and from organic anions such as acetates and formates.

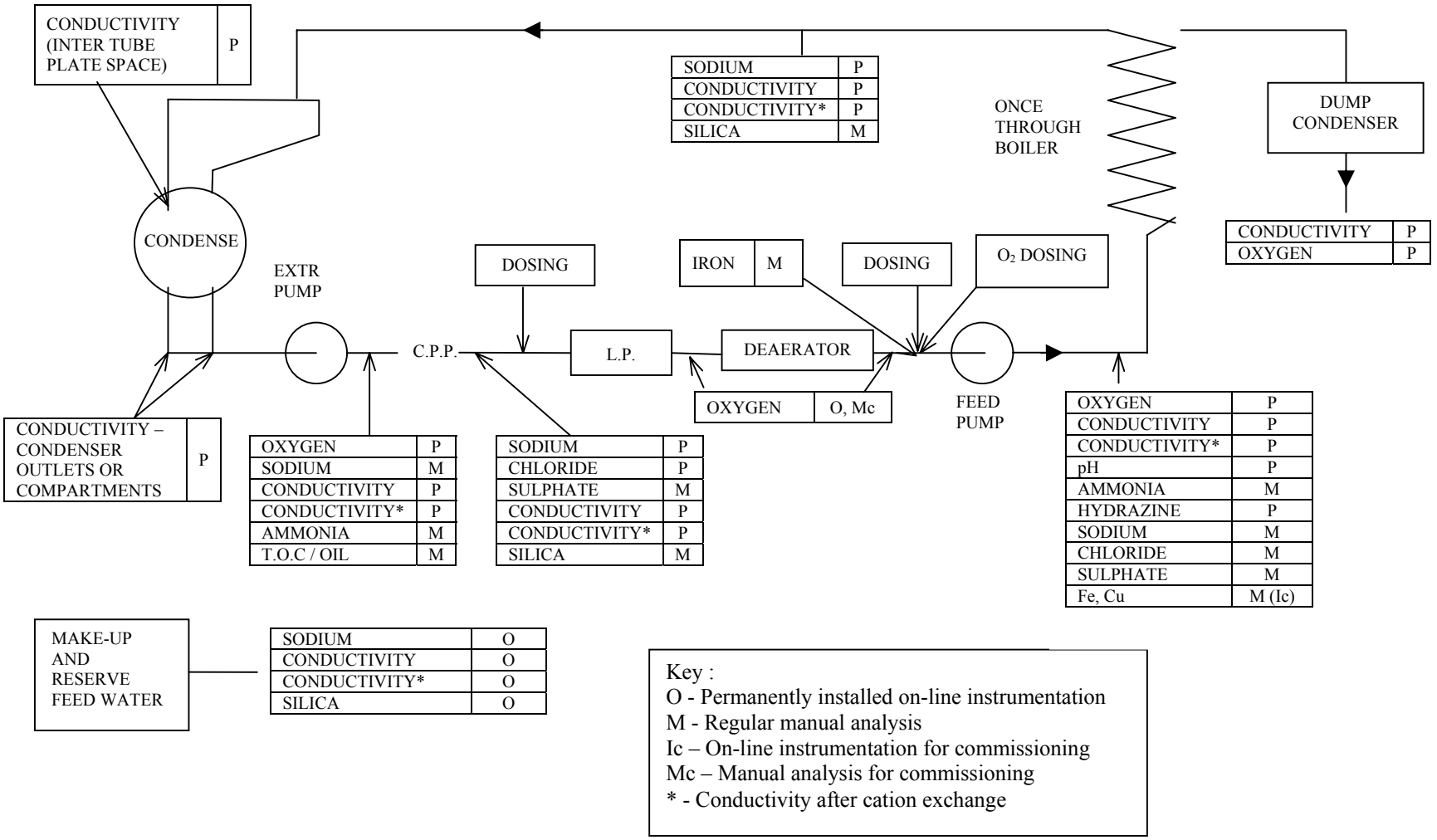

Figure 4. Location of principal sampling and dosing points and analytical requirements (manual or instrumental) for AGR once-through unit[10].

Sodium

The presence of sodium in the steam poses a risk of deposition of alkalis and/or salts[11]. Stress corrosion cracking of turbine steels may occur if highly concentrated alkaline solutions form on the surface. Sodium chloride and sodium hydrogen sulphate also constitute a stress corrosion cracking risk to turbine components.

Silica

Silica has been considered as inactive to corrosion. However, silica in the steam can result in deposition on turbine blades and hence reduce turbine efficiency.

Chloride

Chloride is one of the most corrosive contaminants in the turbine. Chloride of a concentration of 100 ppb has a significant detrimental effect on pitting, which may act as precursors to environment assisted cracking.

Sulphate

Sulphate is another anionic impurity which can contribute to corrosion related turbine failures.

Iron and copper

The main hazards associated with a high level of iron oxide in the steam are solid particle erosion of the initial turbine stages and deposits, with subsequent blockage, of turbine inlet valves.

The main detrimental effect associated with high level of copper in steam is a loss of output due to deposit accumulation. This parameter is only relevant in plant with a copper alloy condenser or feed-water tubing.

Oxygen

A number of surveys have revealed a consistent relationship between the cracking incidence at plants and the presence of oxygen.[15-17] Oxygen can have an important role in pitting and crack initiation. The limiting value of dissolved oxygen in steam is set normally less than 5 ppb but can be up to 25 ppb[14] and 50 ppb[10] in oxygenated treatment.

Tables 1 and 2 list the chemical control targets for drum-type and once-through boilers respectively for the fossil fired, AGR, pressurised water reactor (PWR) and Magnox stations. It can be seen that the chemistry of the once-through steam/water circuit is controlled much more rigorously than that of the drum-type for the reasons explained earlier.

The limits of steam impurities under normal operating conditions set by International Electric Committee (IEC)[14] are listed in Table 3. In addition, the limit values of chloride and sulphate are set as 3 μg/kg (ppb).

Table 1 Chemical control targets for drum-type boilers (Expressed as μg/kg)[10,18].

Water type	Parameter	Boiler class		
		Coal-fired (160 bar)	Magnox	PWR
Feed water	Conductivity (μS/cm at 25 °C)	LD	LD	6.5-7.2
	Na	LD	LD	/
	SO_4	LD	LD	/
	O_2	<5	<5	/
	N_2H_2	LD	LD	/
	NH_3	2 × dissolved O_2 concentration	2 × dissolved O_2 concentration	/
	pH (25 °C)	8.8 – 9.2	8.8 – 9.2	/
Boiler water	Cl	<1000	<1000	<0.1
	SO_4	LD	LD	0-0.2
	NaOH	1.5 × NaCl (min. 2000)	1.5 × NaCl (min. 2000)	/
	Na_2HPO_4/Na_3PO_4	NA	min. 1000	/
	Na	/	/	<0.1
	Cation conductivity (μS/cm at 25 °C)	/	/	0.1
	NH_3	/	/	1000-1100

LD: Local Decision.

Table 2 Chemical control targets for once-through boilers (Expressed as μg/kg, conductivity: μS/cm at 25 °C)[10].

Parameter	Sampling points (See note)	Boiler class					
		AGR		Magnox (Sub-critical)		Supercritical	
		Low Oxygen	Oxygen Dosed	AVT	Oxygen dosed	AVT	Oxygen dosed
pH at 25 °C	BI	>9.3	>9.0	9.2-9.6	>9.4	>9	8.4-8.7
NH_3	BI	>300 depending on pH		As required to meet the recommended pH with an upper limit of 2000 (μg/kg)			
Conductivity direct	Make-up			<0.2	<0.2	<0.2	<0.2
	BI	>2.8	depending on pH	≥4.3	>7.0	>3.5	0.8-1.4
	BO	>2.8		/	/	/	/
	EPD	>2.8		/	/	/	/
	CPPO	>0.08		<0.1	<0.1	<0.1	<0.1
N_2H_2	BI	1.5 × O_2 with minimum of		2 × O_2 min. 10	0	2 × O_2 min. 10	/
		10	40				
	BAO			/	/	/	50
O_2	BI EPD	<5.0 <50	< 25 (LD) <50	<5 <50	10-30 <50	<5 <50	130-200 <50
Na	BI BO CPPO	<2.0 <2.0 <2.0		<5 <5 <5	<5 <5 <5	/ / <5	/ / <5
Cation conductivity	BI BO EPD CPPO	<0.08 <0.08 <0.30 <0.08		<0.1	<0.1	<0.1	<0.1
Cl	BI CPPO	<2.0 <2.0		<2	<2	<2	<2
SO_4	BI CPPO	<2.0 <2.0		<2	<2	<2	<2
SiO_2	BI CPPO	<220 <5					
Fe	BI	<5		<25	<25	<10	<10
Cu	BI	<2		<25	<25	<3	<3
Oil/TOC	BI	/	/	/	/	<100	<100

Note: 1. Sampling points:

CPPO - Condensate polishing plant outlet
BI - Boiler inlet
BO - Boiler outlet
EPD - Extraction pump discharge
DAO - Deaerator outlet

.

Table 3 Steam purity limits for steam turbines, key parameters[14].

Parameter	Expected range	Limit value	Action within 1 week	Action within 24 hours	Action within 1 hours
Conductivity (μS/cm, 25 °C)	0.06 – 0.2	≤ 0.2[a,b]	0.02 – 0.5[c]	0.5 – 1.0	≥1.0
Sodium (ppb)	0 – 5[c]	≤ 5[c]	5 - 15	-	-
Silica (ppb)	3 – 5	≤ 20	-	-	-
Iron[e] (ppb)	2 –5	≤ 20	-	-	-
Copper[f] (ppb)	0 - 1	≤ 3	-	-	-

a For conventional phosphate dosing, a limit value of 0.3 μS/cm may be applied, providing it can be shown that the dominant contribution to the additional conductivity is due to the phosphate ion.
b A higher value may be acceptable when an organic oxygen scavenger or volatile pH conditioner is used, provided that it is shown, for example by analysis of chloride and sulphate, that the increase is not due to aggressive contaminants.
c If chloride exceeds 20 μg/kg, action within 24 hours is necessary.
d Values depend boiler dosing. 5 μg/kg normally attainable as a limit value under AVT. In some plant, up to 10 μg/kg may be appropriate under sodium compound dosing.
e May not need to be monitored in all cases.
f Only monitored in plant with copper alloy heat exchanger tubing, particularly high pressure boiler systems.

The temperature, pressure, and moisture distribution in relation to the location of disc cracking

Fossil-fired power plants

The distribution of steam temperature and pressure varies from station to station, depending on the turbine design and operating conditions. Typical inlet and outlet temperatures and pressures of steam for a fossil-fired steam turbine with a rated output of 500 MW at full load condition[19] are listed in Table 4.

The temperature distribution at disc bores of the LP turbine under full load is shown in Figure 5. It can be seen that condensation starts to occur at approximately 90 °C (where the metal surface temperature is below the saturation point of the steam at the given pressure), assuming a choked flow at outlet end (which is representative of modern “keyway-less” designs). The temperature of the main steam is not shown in Figure 5 but should be similar to the metal surface, if there is no heat transfer to the metal from other sources. However, it should be noted that the metal temperature at disc bores near to the gland seal is higher than the temperature of the main steam and the saturation temperature, due to heat transfer from the sealing steam. In this case,

water droplets may still form on the metal surface as the main steam is wet, but evaporation occurs to prevent the build-up of the liquid film. It appears that SCC would be more likely under this condition, as wet/dry cycles of the metal surface occur and deposits of impurities form. However, SCC of discs and blades in this region has not been reported so far. It is believed[9] that the reason SCC has not occurred is due to insufficient condensation on the metal surface on-load, although there is concern that concentrated impurities may form in the condensate during off-load periods.

Table 4 The typical inlet and outlet temperatures and pressures of steam for a fossil-fired steam turbine with a rated output of 500 MW at full load condition[19]. The pressure is defined as bar, absolute (1 bar = 0.1 MPa).

Turbine	Inlet			Outlet		
	Temperature (°C)	Pressure (barA)	Steam wetness	Temperature (°C)	Pressure (barA)	Steam wetness
HP	564	151.67	/	363	42.05	/
IP	564	37.57	/	230	3.10	/
LP	229	3.03	/	30	0.04	8%

Stress corrosion cracking of turbine steels occurs in many locations[4], as shown in Figure 6. It has been suggested[15,16,20] that disc cracking occurred at or downstream of the Wilson line (locations where the steam moisture is 3 - 4%) in the turbine, suggesting that moisture (or liquid phase) was essential for cracking, whist others state[4-6] that the early condensates (which can form at moisture of less 1%) are more important.

Figure 7 shows an example calculation for the metal temperatures at the keyway crowns of a Marchwood LP rotor and the incidence of cracking. It is clear that cracking, is closely related to the occurrence of condensation on the discs[21].

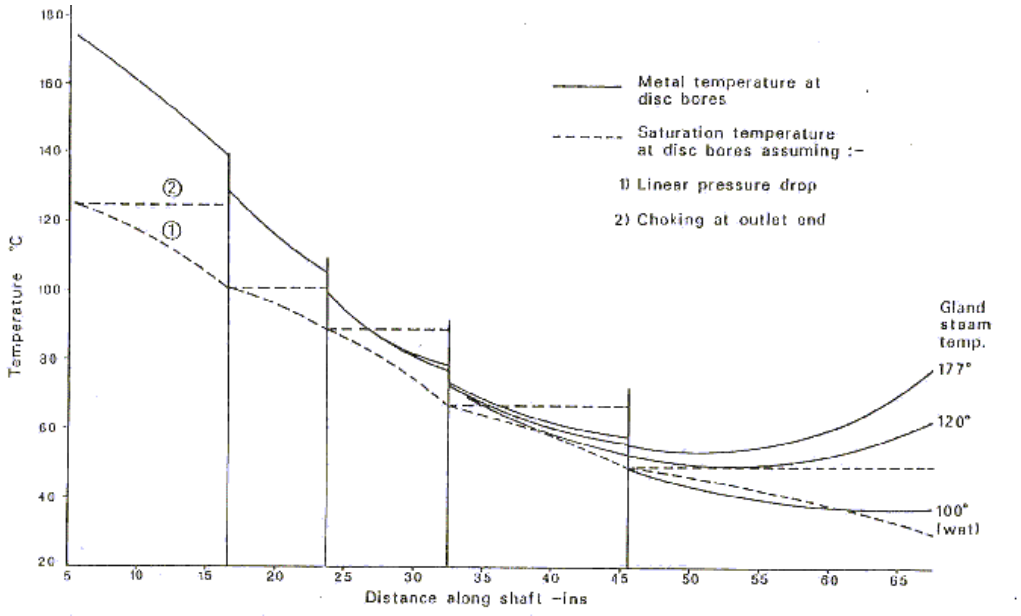

Figure 5. Temperature distribution of a 500MW LP turbine under full load[9].

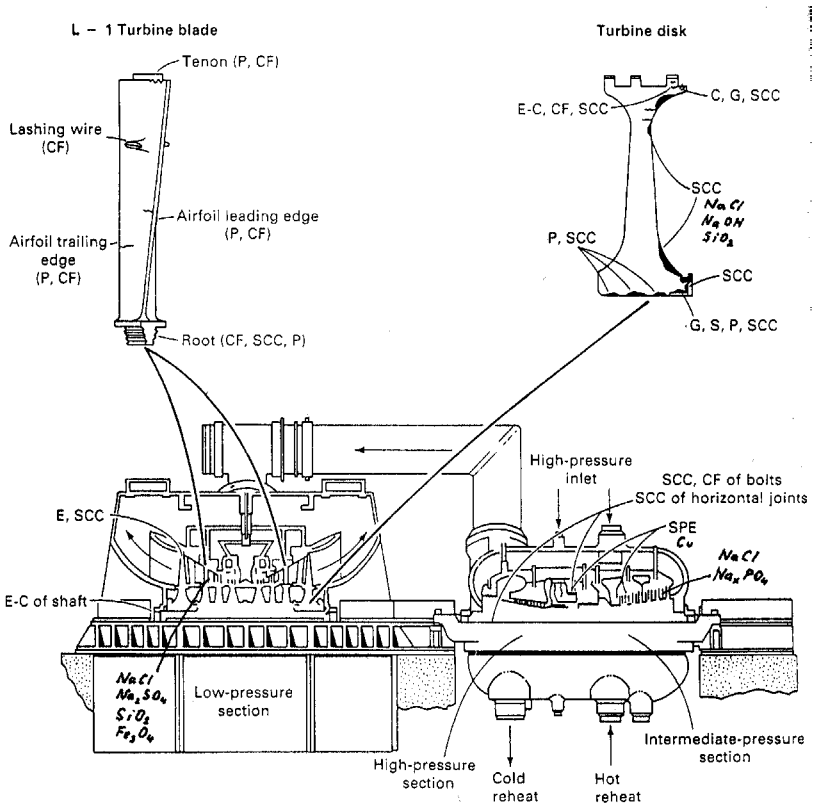

Figure 6. Typical locations of turbine corrosion, erosion and deposits[4]. P. pitting, CF, corrosion fatigue, SCC, stress corrosion cracking, C, crevice corrosion, G, galvanic corrosion, E, erosion, E–C, erosion-corrosion, SPE, solid particle erosion, chemical deposits.

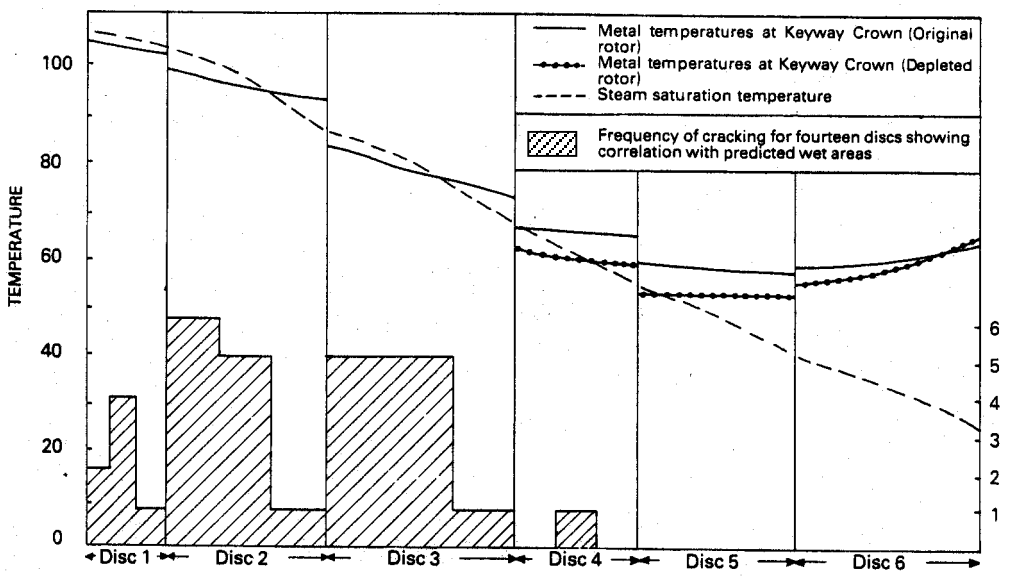

Figure 7. Keyway temperature for Marchwood PS 60 MW LP rotor in its original condition and as depleted (Stage 1, 2 and 3 discs removed), showing UK experience of SCC in steam turbine discs[21].

Nuclear power plants

There are three types of nuclear power stations used in the UK, viz. AGR, Magnox and PWR. The distribution of temperature, pressure and steam wetness are significantly different depending on the type of reactor, as discussed below.

- AGR

The typical operating conditions of the AGR nuclear steam turbines[22] are listed in Table 5. It can be seen that the steam in HP and IP turbines is dry and that condensation only occurs at or after stage 4 of the LP turbine, where the steam temperature is at or below the saturation temperature at the given pressure, i.e. at a temperature of 90 °C or less.

Table 5 The design temperature, pressure and steam wetness distribution in the Hartlepool Unit 1(AGR) turbines[22]. The pressure is defined as bar, absolute (1 bar = 0.1 MPa).

Turbine	Stage	Temperature (°C)	Pressure (barA)	Wetness (%)
HP	1	485	155.00	/
	2	469	140.80	/
	3	454	128.20	/
	4	439	116.60	/
	5	423	105.70	/
	6	408	95.76	/
	7	393	86.50	/
	8	377	77.56	/
	9	359	68.61	/
	10	340	59.82	/
	11	320	51.31	/
	Exhaust	299	43.50	/
IP	1	523	36.60	/
	2	489	29.41	/
	3	453	23.44	/
	4	417	18.36	/
	5	378	14.08	/
	6	338	10.54	/
	7	297	7.67	/
	Exhaust	254	5.40	/
LP	1	266	5.14	/
	2	208	2.80	/
	3	151	1.43	/
	4	90	0.69	/
	5	68	0.29	3.3
	6	49	0.12	6.2
	Exhaust	31	0.05	9.6

- PWR

The PWR is operated under vary different conditions[22], as shown in Table 6. The HP turbine is almost all wet and the Wilson line temperature is above 250 °C. The LP turbine is partly wet and the Wilson line is at less than 78 °C. It should be noted that SCC of HP turbine discs and blades has not been reported, despite condensation occurring at very high temperature. This is probably due to the fact that the loading level of HP turbine discs and blades is much lower than that of the LP turbines.

Table 6 The temperature, pressure and steam wetness distribution of Sizewell B Unit1(PWR) turbine[22].

Turbine	Stage	Temperature (°C)	Pressure (barA)	Wetness (%)
HP	1	283	66.77	0.3
	2	250	40.00	5.9
	3	224	25.10	9.0
	4	201	15.80	11.6
	5	179	9.70	13.7
	Exhaust	157	5.70	15.3
LP	1	273	5.65	/
	2	200	2.60	/
	3	132	1.10	/
	4	78	0.43	0.6
	5	53	0.14	5.4
	Exhaust	30	0.04	9.3

- Magnox

The distribution of temperature, pressure and wetness of the steam in the Magnox power plants is not available. There is a large variation in the temperature and pressure of the inlet and outlet steam from station to station[23], as indicated by the typical operating data for four stations shown in Table 7. It can be seen that the Magnox stations operate under much lower pressures compared to AGR and PWR. It has been suggested[23] that the temperature at which first condensation occurs at the Magnox stations is in the range 70 °C to 120 °C for the LP turbines and about 170 °C for the HP turbines.

Table 7 The temperature and pressure range of the inlet and outlet steam in turbines at four Magnox stations[23].

Turbine	Steam	Temperature (°C)	Pressure (barA)	Wetness (%)
HP	Inlet	325 - 358	22.5 - 38	/
	Exhaust	102 - 120	1.1 – 1.9	2 – 9
LP	Inlet	The temperature and pressure are close those at the HP exhaust, except in one station in which the temperature is 187 °C as the steam is reheated before entering the LP.		0 - 3
	Exhaust	22 - 23	0.03 – 0.05	8 - 14

Temperature for the first condensation and thickness of condensate layer

The distribution of temperature and pressure in the turbines is complex and varies from station to station, as described above. Therefore, it is not possible to make general statements on the distribution of steam moisture content in the turbine and hence the exact location where condensation starts to occur. The temperatures at which the first condensation occurs in the LP, IP and HP turbines for various stations in the UK are summarised in Table 8. However, it should be noted that there are variations in the distribution of temperature and pressure in the turbines during operation, especially during start-up and shutdown period. Therefore, the Wilson line may move. Hence, there are locations that will experience cyclic dry/wet steam conditions. Furthermore, early condensate could form above the saturation temperature due to local supercooling of the steam flow and the presence of impurities[5].

Table 8 The temperatures at which first condensation occur in the LP, IP and HP turbines for various stations.

Type of station	Saturation temperature (°C)		
	LP	IP	HP
Fossil-fired	< 100	No condensation	No condensation
AGR	< 90	No condensation	No condensation
PWR	< 78	N/A*	250 - 280
Magnox	70 - 120	N/A*	~ 170

* N/A: Not applicable.

The thickness and continuity of the liquid film depend on the steam moisture content, chemical impurities, wettability and rotation speed of the surface where the film is located [5,6,24]. Film thicknesses of up to 120 μm have been measured in model turbines at MEI[6]. An EPRI[24]study revealed that at steam moisture less than 1%, no continuous liquid film forms on the turbine components in the steam flow path. However, early condensates form at moisture levels of less than 1%.

Impurities on the Surface of Blades and Discs

Source of impurities in steam

As described above, the boiler and feed-water chemistry is tightly controlled under normal operating conditions. However, high levels of impurity in the feedwater and boiler water may arise during chemical excursions due to: (a) the deficiency of water treatment (e.g. demineralisation and deaeration equipment failure); (b) leakage from the condenser; (c) transient in water chemistry during start-up and shutdown period; (d) contamination of corrosion products in the boiler, feed-water tubing, etc.

Impurities can be transported into the steam in at least three ways, as described below.

- At a high temperature and pressure, salts can be dissolved in dry steam (vaporous carry-over). The solubility of salts in steam is a function of steam pressure, temperature and the partition coefficient (the ratio of the concentration of the salt in steam to that in the water). The solubility of corrosive salts in steam has been

studied extensively[3,4]. The partition coefficient has been found to be typically in the range of 10^{-3} to 10^{-4} and increases with temperature and pressure.

- The impurity can also be transported into the steam by entrainment of droplets of boiler water (mechanical carry-over).

- The impurity may result from injection of feedwater into steam for superheat/reheat temperature control and leakage of boiler water into superheated steam in tubular desuperheaters[7,10].

When the steam enters the turbine, the impurities from the steam can be transported onto the metal surface by deposition (vapour to solid) and condensation (vapour to liquid). The deposits can be formed on the LP turbine, as well as on the HP and IP turbines, especially during major chemical excursions. Early condensates form even when the steam wetness is less 1% due to the local supercooling and presence of impurities[6]. When the steam wetness is above 1%, a continuous liquid film may form on the turbine surface. The impurities formed on the surface of blades and discs reduce the turbine efficiency and cause pitting, erosion and stress corrosion cracking, as shown in the Mollier diagram[4].

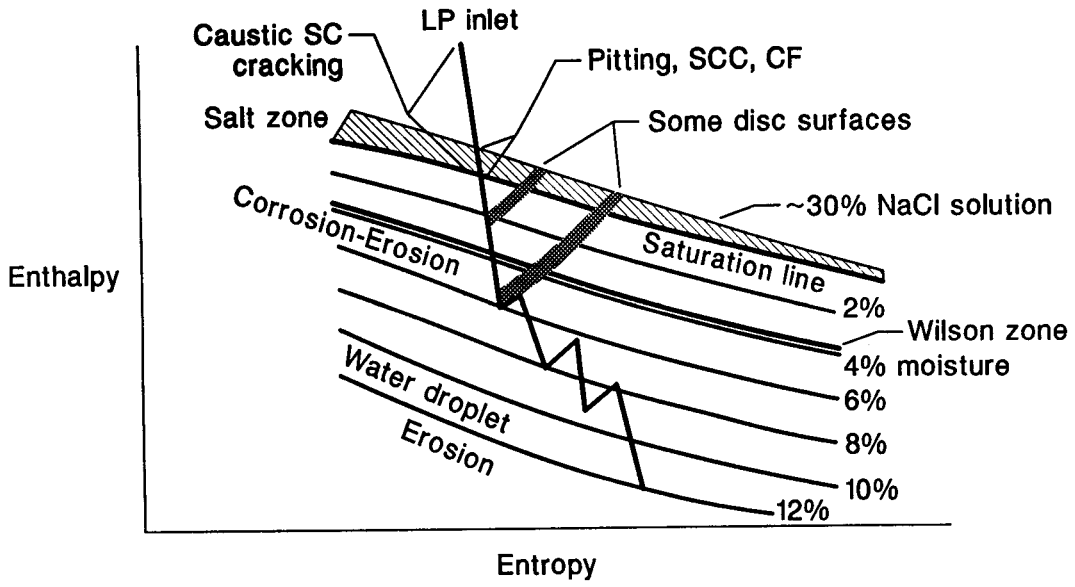

Figure 8. Mollier diagram showing regions of deposition and condensation and their effect on corrosion[4].

The concentrations of corrosive impurities, e.g. chloride, oxygen and carbon dioxide, that may be obtained in the liquid films, early condensates and deposits, are now assessed.

Impurities in liquid films

The concentration of impurities in the water phase can be calculated using thermodynamic data,[25,26] assuming that the impurities in the vapour (steam) and liquid (condensate) phase is close to equilibrium[27].

Chloride

Two assumptions are made:

- Chloride salts are the sole contaminants of the steam;
- All chloride salts are partitioned into the water phase;

In these conditions, the chloride concentration in the steam can be derived from the measured cation conductivity of the condensed steam (hence the solution after cation exchange is dilute HCl) as follows.

$$\lambda_{steam} = \lambda_{HCl} + \lambda_{dissociated\,water} \quad (1)$$

and

$$\lambda_{steam} = \alpha_{HCl} x + \alpha_{dissociated\,water} y \quad (2)$$

where α_{HCl} and $\alpha_{dissociated\ water}$ are the conductivity coefficients of HCl and dissociated water (μS/cm per mol/l), x = $[Cl^-]$ and y = $[OH^-]$. If z =$[H^+]$, we have

$$zy = K_w \quad (3)$$

and

$$z = x + y \quad (4)$$

or

$$x = \frac{K_w}{y} - y \quad (5)$$

where K_w is the water dissociation constant.

Since x is the concentration of chloride (mol/l) or the number of moles in 1 kg steam, then

$$c_{Cl^-,steam} = 35.5 \times 10^{-3} \times 10^6 x = 3.55 \times 10^4 x \quad (6)$$

$c_{Cl,\,steam}$ is the chloride weight concentration in the steam (ppm).

Assuming all the chloride is partitioned in the water phase, then,

$$c_{Cl^-,water} = \frac{c_{Cl^-,steam}}{y_n} \quad (7)$$

where y_n is the wetness.

Combining Equations (2) and (5), we have

$$ay^2 + by + c = 0 \qquad (8)$$

where $a=\alpha_{HCl} - \alpha_{dissociated\ water}$, $b = \lambda_{steam}$ and $c = -(\alpha_{HCl}k_{water})$

From Equation (8), we obtain (as y should be a positive value)

$$y = \frac{-b + \sqrt{b^2 - 4ac}}{2a} \qquad (9)$$

At 25 °C, $\alpha_{dissociated\ water} = 5.5 \times 10^5$ (μS/cm)/(mol/l), $\alpha_{HCl} = 4.3 \times 10^5$ (μS/cm)/(mol/l) and $K_w = 10^{-14}$. From Equations (5), (6), (7) and (9), the chloride content in the water phase can be calculated at various values of steam conductivity and steam wetness, as shown in Figure 9.

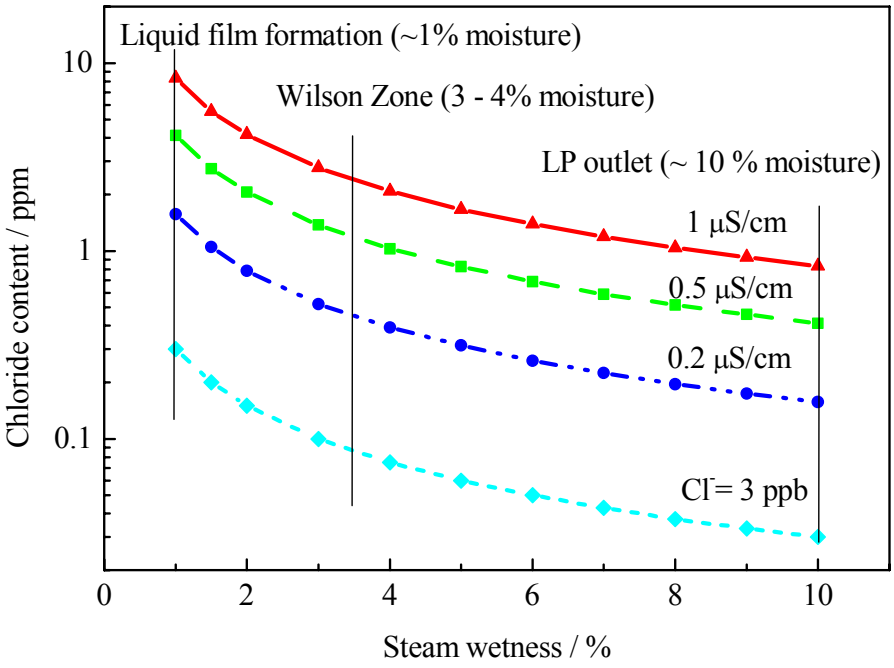

Figure 9. Chloride content in the water phase as a function of steam wetness at various cation conductivities of the inlet steam.

It can be seen that the chloride concentration in the liquid phase at 1% of moisture, at which a continuous liquid film may form, is 1.6 ppm under normal operating conditions (cation conductivity of the steam equal to 0.2 μS/cm) and can be as high as 10 ppm during a chemistry excursion (cation conductivity equal to 1 μS/cm). At the Wilson line where the moisture content is 3 – 4 %, the chloride concentration in the liquid film is approximately 0.45 ppm, 1.2 ppm and 2.4 ppm when the cation conductivity of the steam is 0.2 μS/cm, 0.5 μS/cm, 1.0 μS/cm respectively. However,

it should be noted that the data shown in Figure 9 represent the upper boundaries of chloride in the liquid phase, as the chloride salts are assumed as the sole contaminants in the steam. On this basis, for example, a cation conductivity of 0.2 μS/cm (25 °C) would correspond to approximately 15 ppb of chloride. It is stated in the water chemistry guideline[14] that a steam cation conductivity of 0.2 μS/cm should never be allowed to consist of so much chloride and the limiting value has been set to 3 ppb. The chloride concentration in the liquid film for the steam containing 3 ppb chloride is also shown in Figure 9 from which it can be seen that the chloride in the condensate is predicted to be 300 ppb and 100 ppb for the steam wetness of 1% and 3% respectively.

Higher chloride concentration may exist in the regions where the steam is dry or where wet/dry cycles occur, as will be discussed later.

Other non-volatile species

In the section above, only chloride contamination in the condensate was discussed. However, the conclusion derived can be applied to other non-volatile species, viz. the maximum concentration of non-volatile species in the liquid phase is 100 times higher than that in the steam phase, if the liquid film can form on the turbine surface at a moisture level of 1%. For instance, a solution with a cation conductivity of 0.2 μS/cm (25 °C) would correspond to approximately 20 ppb of sulphate ion as the only anion[14]. Therefore, the maximum concentration of sulphate in the liquid phase would be 2 ppm. If the sulphate concentration in the steam were controlled at less than 3 ppb under normal operating conditions, the maximum concentration of sulphate ion in the liquid phase would be 300 ppb.

Recently, the presence of organic species, such as acetates and formates, in the steam has increasingly become a concern. In nuclear power stations, the total organic compounds (TOC) are controlled below 100 ppb[28]. The presence of organic acid, such as acetic acid, which may form in the condensate if the acetate ions are not balanced by cations, would significantly reduce the pH of the condensate and result in general corrosion, pitting and environment assisted cracking. For example, if the acetate ion concentration in the steam were 100 ppb and all acetate ions were partitioned in the liquid phase, the maximum concentration of the acetate ion in the condensate would be 10 ppm. If the acetate ion at a concentration of 10 ppm were to form acetic acid, the pH of the condensate would be reduced to 4.3 at 90 °C. However, further work is needed to establish more reliably the concentration of acetate in the steam and the state of acetate compounds (acid or salts).

Oxygen

The following assumptions are made in calculating the oxygen concentration in the condensate:

- There is no air carried over by the steam and there is no leakage of air into the steam turbine. Therefore, the only source of oxygen contamination is the dissolved oxygen in the feedwater.

- The steam pressure at a given temperature is equivalent to the equilibrium pressure of water vapour. This is a reasonable assumption at the saturation temperatures where condensation occurs (Tables 5 and 6).

The oxygen content in the water phase, $c_{oxygen,\ water}$, can be expressed as

$$c_{oxygen,water} = \alpha_{oxygen} \times p_{oxygen} \quad (10)$$

where p_{oxygen} is the partial pressure of oxygen in the steam and α_{oxygen} is the solubility of oxygen in the water at a given temperature.

The partial pressure of oxygen in the steam can be written as

$$p_{oxygen} = c_{oxygen} \times p_{steam} \quad (11)$$

where p_{steam} is the steam pressure and c_{oxygen} is the oxygen content in the steam.

The oxygen content in the water phase as a function of temperature at various oxygen concentrations in the inlet steam are shown in Figure 10. It can be seen that the oxygen content in the water phase is less than 1 ppb even when the inlet steam contains 8 ppm oxygen, as long as there is no presence of air in the steam. The calculation is in agreement with the experimental data measured in the condensate[5] (see below).

There is a concern that air may be present at locations where the temperature is low and the steam pressure is less than the atmosphere pressure (under vacuum) when air leakage from the gland seal occurs. Since the air content due to leakage is not known, the oxygen content in the water phase is plotted in Figure 11 as a function of temperature at various partial pressures of air. The partial pressure of air due to leakage is expected to be very low, as the velocity of the steam flow is high. Nevertheless, it can be seen from Figure 11 that high levels of oxygen may exist in the water phase when excessive air leakage occurs.

Another source of oxygen contamination is leakage of the condenser. The cooling water may spread directly on the blades and discs. In this case, the oxygen concentration in the liquid phase would be close to the dissolved oxygen level in the cooling water.

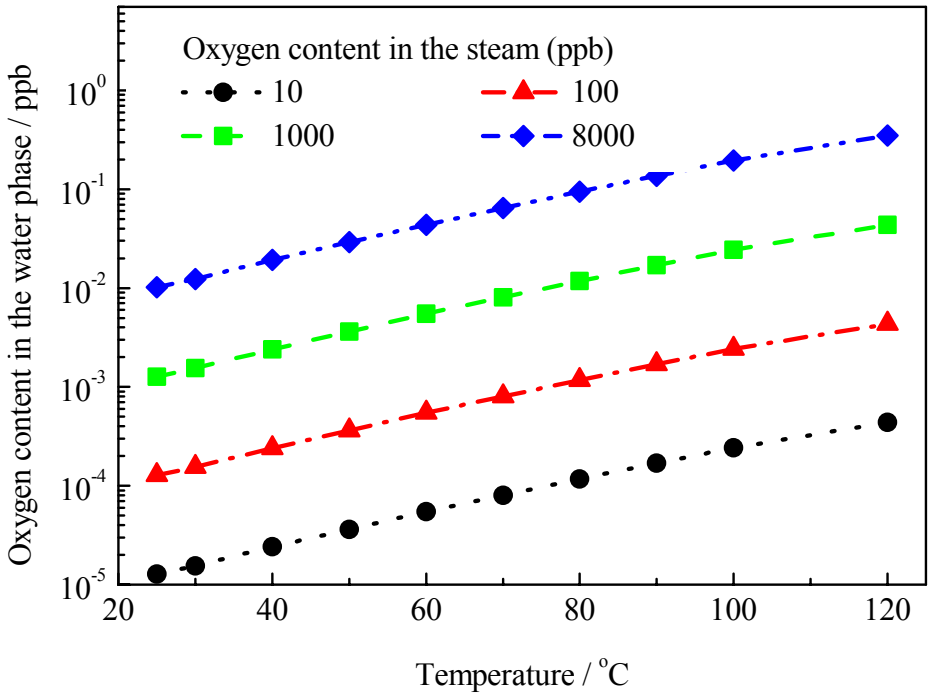

Figure 10. The oxygen content in the water phase as a function of temperature at various oxygen concentrations in the inlet steam.

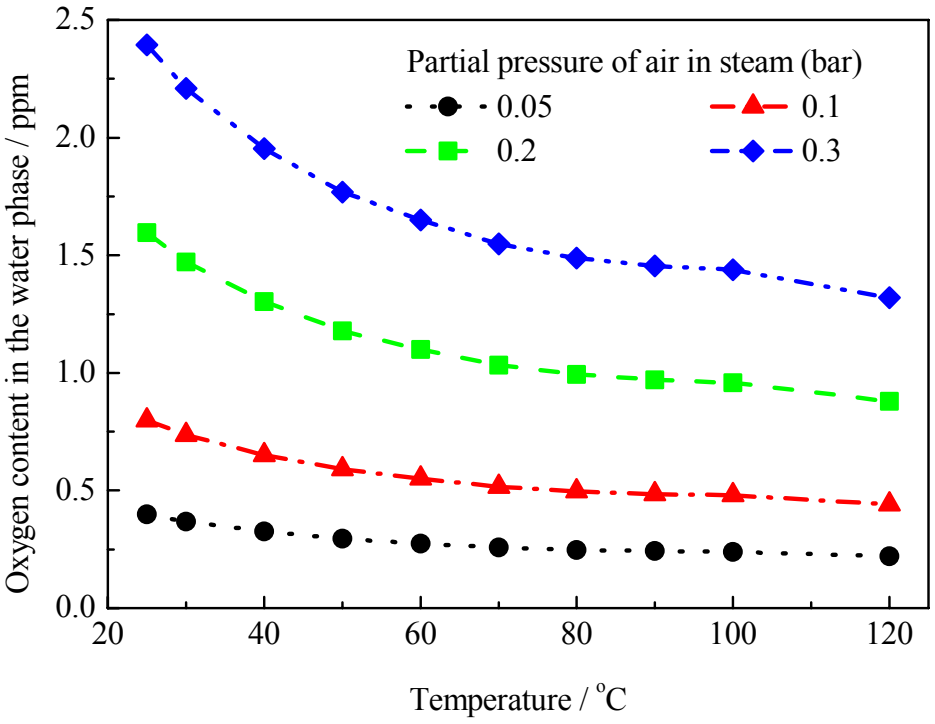

Figure 11. Oxygen content in the water phase as a function of temperature at various partial pressures of air in the inlet steam.

It should also be noted that the calculation above is applicable only to isothermal solubility equilibrium, i.e. to systems characterised by sufficiently high two-phase mass flows on both the supply and the exhaust side and by quasi-constant temperature. At non-equilibrium conditions, there are deviations resulting in higher concentrations of gaseous species (e.g. oxygen and carbon dioxide) in the liquid phase. In the extreme case of so-called "forced condensation", where all of the steam is forced to condense to water in the turbine rather than being exhausted, the concentration of gaseous species in the condensed liquid layer on the turbine steel can be similar to that in the supply steam[4].

The effect of the relative exhaust steam (ratio of the exhaust steam flow to the inlet steam flow) on the partitioning of gaseous species can be illustrated by the partitioning of oxygen. Figure 12 shows the oxygen concentration in the condensate partitioned from the steam containing 18 ppm oxygen at 283 °C and 184 °C as a function of the relative exhaust steam flow[4] (the reason for the choice of 18 ppm oxygen was not explained). At near 100% exhaust steam flow, the concentrations of oxygen in the condensate are consistent with those calculated based on an equilibrium system. When the relative exhaust steam is close to zero, the oxygen concentrations in the condensate approaches the value in the inlet steam.

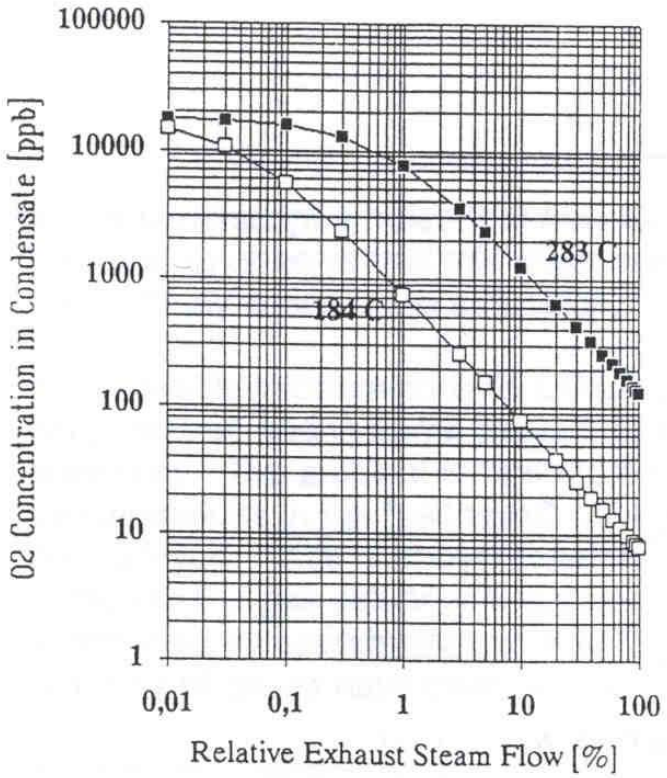

Figure 12. The effect of exhaust steam flow on the dissolved oxygen in the condensate at 184 °C and 283 °C (inlet steam contains 18 ppm oxygen)[4].

Depletion time for oxygen from the condensate layer during start-up

When the steam turbine is on-load, the gland is sealed with the gland steam. Off-load, the gland steam is no longer supplied and hence air leakage occurs. Therefore, the condensate may be air saturated, with an oxygen concentration of 7.6 ppm at 30 °C

(off-load during weekend) and 3.7 ppm at 70 °C (off-load overnight). Consequently, there is a period during the start-up when the steam is wet and there is oxygen in the condensate layer. Although the liquid layer is thin and rapid deaeration would be expected intuitively, it is pertinent to demonstrate this.

Mathematically, this is a straightforward problem, assuming the steam itself can be assumed to be oxygen-free upon start-up. The details are described in Appendix 1, which should be viewed in the context of Figure 13.

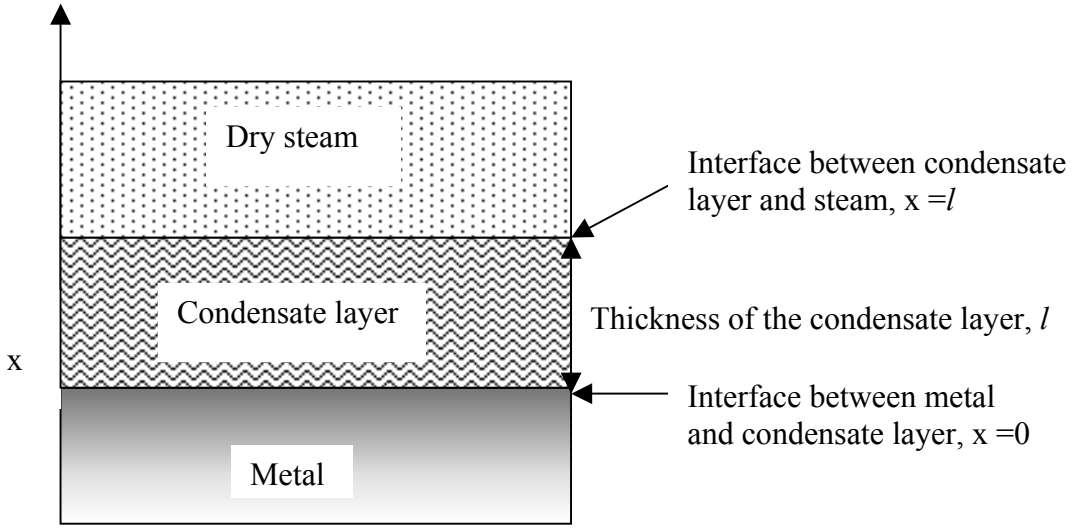

Figure 13. Schematic diagram showing the oxygen diffusion process in the condensate layer.

Figure 14 shows the concentration of oxygen on the metal surface (x = 0) as a function of time at various values of the condensate layer thickness, assuming the initial value of the oxygen concentration is 3.7 ppm (the oxygen concentration in water saturated with air at 70 °C). It can be seen that it takes only 8 seconds for the oxygen concentration on the metal surface to reduce to less than 3 ppb, if the thickness of the condensate layer is 100 μm. (It will take 14 minutes if the layer thickness is 1 mm). Therefore, it may be concluded that the oxygen dissolved in the condensate during the off-load period will be depleted quickly during start-up and should have no significant impact on environment assisted cracking of turbine discs and blades, provided that the oxygen in the steam is oxygen-free.

However, due to the complexity of the turbine structure, the air leaked into the turbine chamber during off-load may take a long period to be removed completely. In-situ electrochemical measurements have suggested that “corrosion activity” of steam turbine blades remains high for several hours during start-up[29].

The chemical excursions during start-up are complex as air leakage, forced condensation, and direct spray of condensed steam on the blade surface (to cool down the metal surface caused by friction as the turbine chamber is not under vacuum during start-up), may all occur. All these processes may lead to a high level of oxygen in the steam and the liquid phase on the metal, which potentially could have an influence on EAC susceptibility.

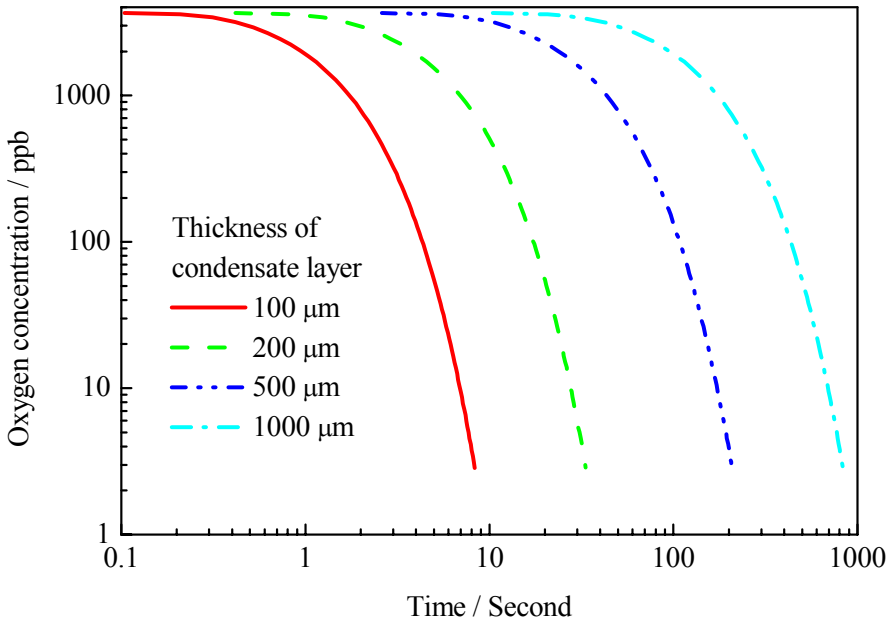

Figure 14. Oxygen concentration on the metal surface (x = 0) as a function of time at various values of condensate layer thickness.

Carbon dioxide

There is some concern in nuclear AGR power plants that contamination by CO_2 in the steam may pose a risk to corrosion and stress corrosion cracking. The ingress of CO_2 into the steam may occur due to leakage of CO_2 coolant in the reheater where the pressure of the steam and CO_2 is about 37.5 bar and 40 bar respectively. The typical concentration of CO_2 in the steam is 5 to 10 ppb and can be up to 1.5 ppm[30]. CO_2 enriched in the liquid film may significantly increase the aggressiveness of the liquid due to the increase of the conductivity and the decrease of the pH.

When CO_2 in the steam and the liquid film reaches an equilibrium state, the concentration in the gas and liquid phases is governed by the following reactions:

$$H_2O = H^+ + OH^-$$

$$K_w = [H^+][OH^-] \qquad (12)$$

$$CO_2\,(g) = CO_2\,(aq)$$

$$K_{CO_2(g)} = \frac{[CO_2(aq)]}{p_{CO_2(g)}} \qquad (13)$$

$$CO_2\,(aq) + H_2O = H^+ + HCO_3^-$$

$$K_{CO_2(aq)} = \frac{[H^+][HCO_3^-]}{[CO_2(aq)]} \qquad (14)$$

$HCO_3^- = H^+ + CO_3^{2-}$

$$K_{HCO_3^-} = \frac{[H^+][CO_3^{2-}]}{[HCO_3^-]} \quad (15)$$

Also

$$[H^+] = [OH^-] + [HCO_3^-] + \frac{1}{2}[CO_3^{2-}] \quad (16)$$

At pH < 7, $[CO_3^{2-}] << [HCO_3^-]$. Hence,

$$[H^+] = [OH^-] + [HCO_3^-] \quad (17)$$

From Equations (12) to (17), we have

$$[H^+] = \frac{K_w}{H^+} + \frac{K_{CO_2(aq)}[CO_2(aq)]}{[H^+]} = \frac{K_w}{H^+} + \frac{K_{CO_2(aq)}K_{CO_2(g)}p_{CO_2(g)}}{[H^+]} \quad (18)$$

or

$$[H^+] = \sqrt{K_w + K_{CO_2(aq)}K_{CO_2(g)}p_{CO_2(g)}} \quad (19)$$

$$pH = -Log\sqrt{K_w + K_{CO_2(aq)}K_{CO_2(g)}p_{CO_2(g)}} \quad (20)$$

The calculated concentration of CO_2 in the liquid film and the effect on pH as a function of temperature at various contents of CO_2 in the steam are shown in Figures 15 and 16. It can be seen that the CO_2 in the liquid film is about 1 ppb if the steam contains 1.5 ppm CO_2. There is no effect of the dissolved CO_2 in the liquid film on pH when the content of CO_2 in the steam is 1.5 ppm. The effect of CO_2 on the pH of the liquid film is still negligible even if the CO_2 content in the steam increases to 10 ppm. The effect of such a low concentration of dissolved CO_2 on the conductivity of the condensates is also negligible.

However, CO_2, like O_2, may have a significant effect on the chemistry of the condensates during chemical excursions, e.g. off-load and start-up. For instance, during the off-load period, the liquid film formed on the turbine surface may be air-saturated due to the air leakage from the gland seal. Based on the thermodynamic data[24,26], the effect of the dissolved CO_2 from atmosphere on the pH and conductivity of condensates can be readily calculated. Figure 17 shows the pH of deaerated and aerated pure water as a function of temperature. It can be seen that dissolution of CO_2 from the atmosphere results in a lower pH in aerated pure water compared to that in deaerated pure water.

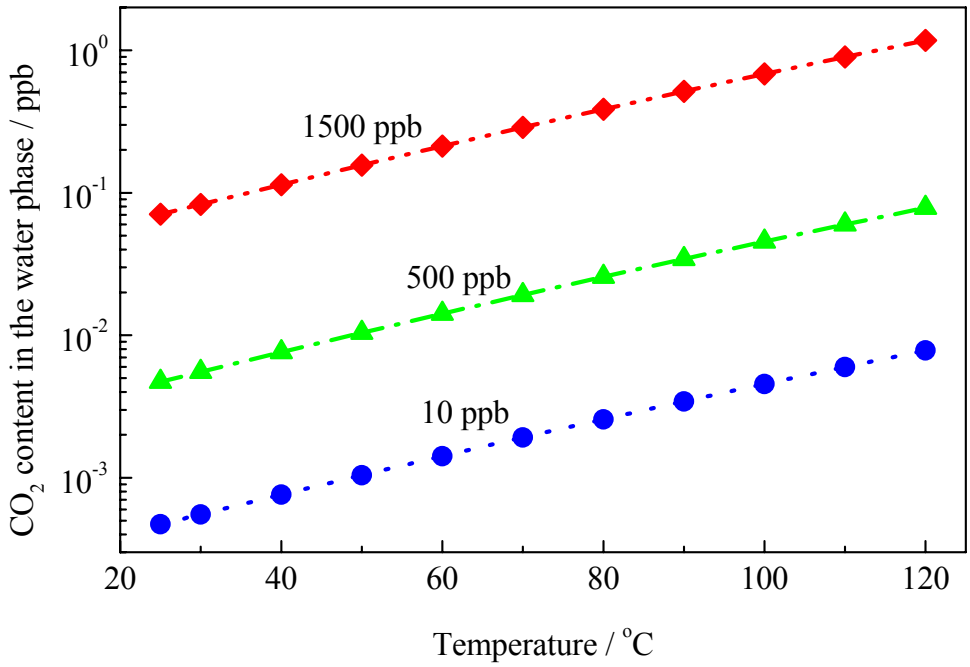

Figure 15. The carbon dioxide content in the liquid phase as a function of temperature at various concentrations in the inlet steam.

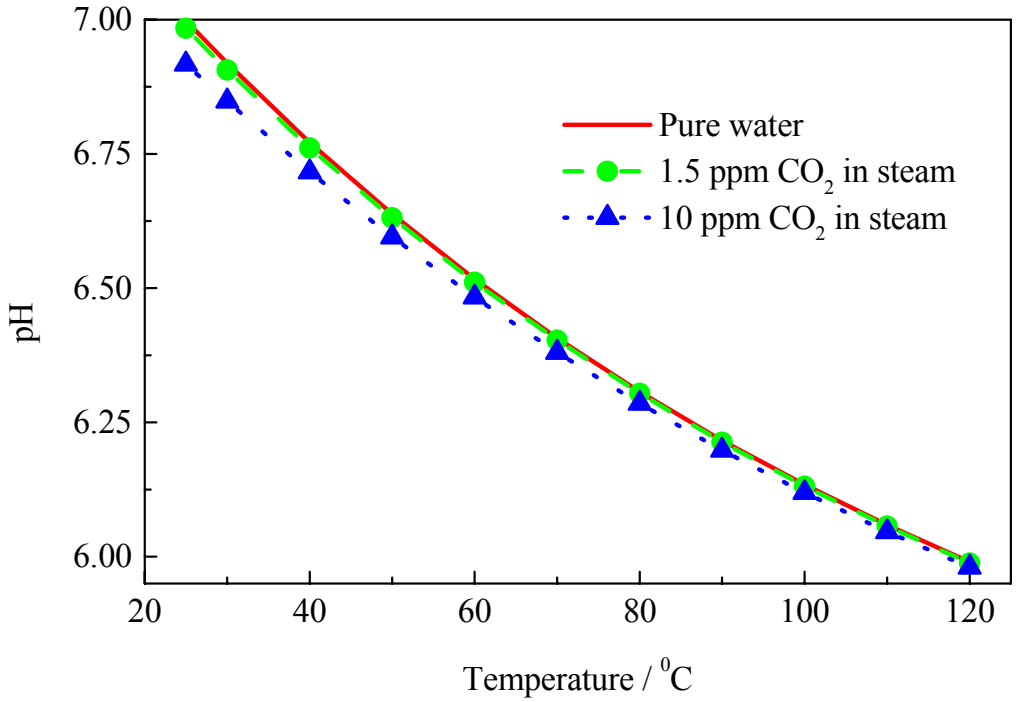

Figure 16. The effect of dissolved carbon dioxide on pH of the liquid phase as a function of temperature at various concentrations in the inlet steam.

The dissolved CO_2 in the condensates during off-load and start-up may also have a significant effect on the conductivity of the liquid films. For instance, the conductivity of deaerated pure water and aerated water is respectively 0.055 μS/cm and 0.89 μS/cm at 25 °C, and 0.53 μS/cm and 0.85 μS/cm at 70 °C. Therefore, an increased susceptibility to EAC, especially crack initiation, might be anticipated as will be discussed in Section 2.

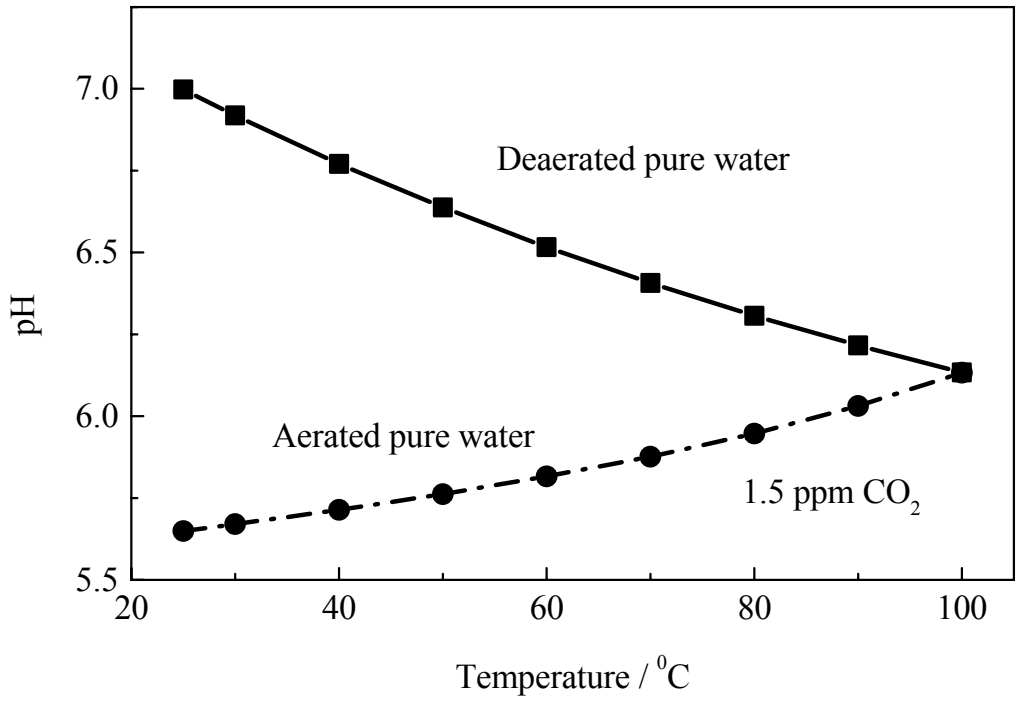

Figure 17 Effect of dissolved CO_2 on the pH of water.

Impurities in early condensates

In the phase transfer region, early condensates (water droplets) can form due to local supercooling of the steam flow[6]. Impurities present in the steam are also the reason for early partial condensation of steam, because the saturation line for soluble impurities is above the phase transition line for pure steam. It has been claimed[6] that the early condensate poses an increased risk to stress corrosion cracking due to the high level of impurity and relatively high temperature.

The concentration of impurities in the early condensate has been studied both theoretically and experimentally[5,6,31,32]. Table 9 and Figure 18 show typical data[24] measured at Moscow Electricity Institute (MEI) using a model power plant. Some key findings are summarised below.

It can be seen that the pH of the early condensate and liquid film is always lower than that of the inlet steam, being near neutral or slightly acidic. This is consistent with the data measured by Vasilennko[31] but is contradictory to the earlier work by Jonas[32] who

analysed the chemistry of the condensed steam from the condenser hot well and suggested that the pH of the condensate was approximately the same as that of the inlet steam. However, the later data may not reflect the chemistry of the water droplets.

At a chloride level in the inlet steam similar to that under normal operating conditions (2 ppb to 3 ppb), the chloride concentration in the early condensate was approximately 100 ppb, which is similar to that measured at real power stations[31]. It should be noted that the chloride concentration is less than that calculated based on the equilibrium data (see previous section), assuming the moisture content is 1% or less (Figure 9). This suggests that the impurities in the steam and the early condensate are not at equilibrium, i.e. there are still some impurities remaining in the steam.

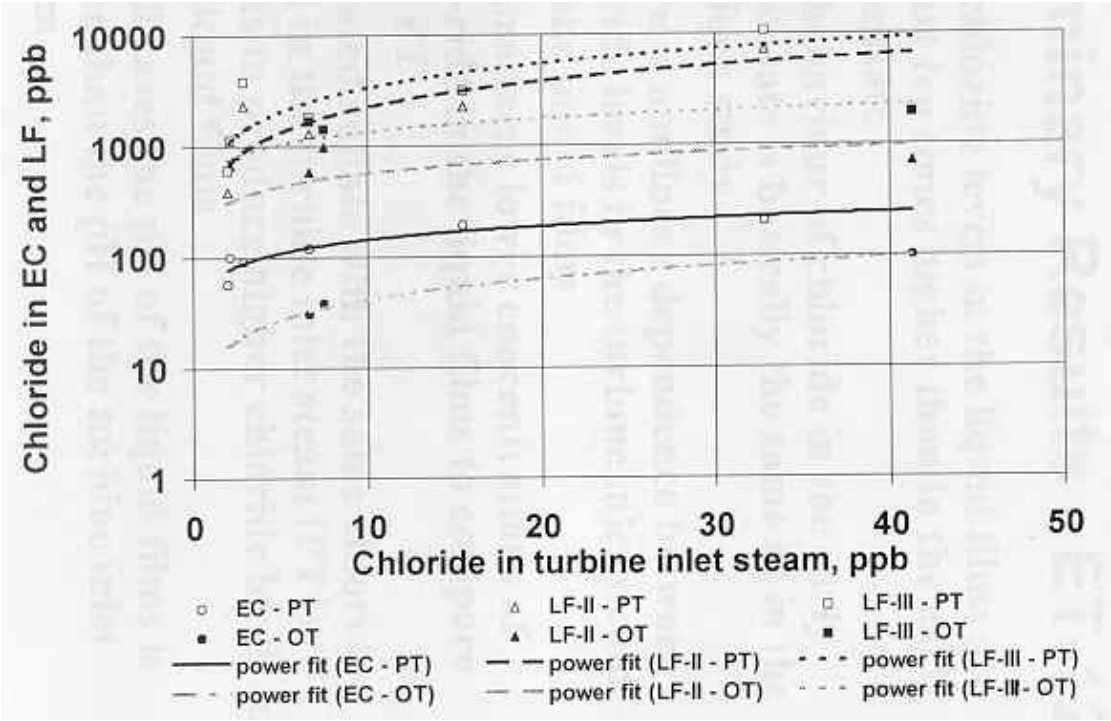

Figure 18. Chloride content in the early condensate and the liquid film as a function of chloride content in the inlet steam (EC: Early Condensate, LF: liquid film, PT: Phosphate Treatment, OT: Oxygen Treatment)[24].

A surprising result was that the measured chloride concentration in the liquid film was higher than that in the early condensate. It has been suggested[6] that the generation of high chloride in the liquid film is due to partial evaporation. However, the authors do not explain why a similar evaporation process would not concentrate the chloride to the same or higher level in the early condensates. The results obtained may reflect the difference between the measurement methods used to collect and analyse the chemistry of the early condensates and of the liquid films. The chloride concentration measured for the liquid film was more variable, in the range of 50 to 1000 times higher than that in the inlet steam.

Table 9 Chemistry of early condensate and liquid film[24].

Chemistry	y_n	Inlet steam		EC		LF II		LFIII	
		Cl^-, ppb	pH	Cl^-, ppb	pH	Cl^-, ppb	pH	Cl^-, ppb	pH
PT	0.78	2.0	9.30	55.8	6.8	385.9	6.3	604.3	6.3
PT	0.90	2.1	9.22	100.0	6.7	672.7	6.1	114	6.1
PT	0.75	2.9	9.35	91.0	6.6	2331	6.5	3811	6.3
PT	0.75	6.7	9.20	118.2	6.3	1300	6.4	1845	6.3
PT + NaCl	0.75	15.5	9.20	191.0	6.8	2296	6.3	3175	6.6
PT + NaCl	0.82	32.8	9.30	205.0	6.9	7191	6.9	10734	6.6
PT*	0.75	2.0	9.28	114.2	6.9	399.0	6.5	2177	6.4
OT	0.76	6.7	8.52	114.1	6.3	582.2	6.3	1678	6.3
OT	0.75	7.5	8.50	30.5	6.3	982.0	6.6	1434	6.3
OT +NaCl	0.76	41.3	8.48	38.5	6.3	709.4	6.3	1928	6.3

During all tests turbine inlet steam pressure p_0 = 0.11 MPa, turbine inlet steam temperature T_0 = 123 C, and Nozzle inlet pressure p_n = 0.05MPa

PT* is the test with elevated sulphate level (23.1 ppb) in the turbine inlet steam

y_n is the steam moisture at the nozzle inlet

EC is the early condensate, LF-II and LF-III are liquid film (sections II and III)

Other inorganic impurities, such as sodium and sulphate, in the early condensate have also been studied[5]. Generally, the concentration factor (the ratio between the impurity concentration in the early condensate and in the inlet steam) is between 10 and 50, i.e. less than that calculated by assuming that all impurities are partitioned in the liquid phase and that the moisture is 1% or less.

Impurities in deposits

The various studies of deposition of corrosive salts on steam turbines have been well documented in recent reviews[2,33]. Generally, it is believed that there are over 150 chemical compounds in millimetre thick deposits with concentrations ranging from a few ppms by weight of deposit to almost 100% of the deposit[33].

There are two major mechanisms for the deposition of impurities on the turbine, i.e. deposition from superheated steam and evaporation of condensate on hot surfaces[33].

- Deposition from superheated steam

When the concentration of a molecular impurity in superheated steam exceeds its solubility under certain pressure and temperature conditions, the impurity starts forming molecular clusters and precipitates, some of which deposit on the turbine surface. Since the solubility of impurities in dry steam decreases as the steam expands, precipitation and deposition is most likely to occur on turbine components operating at the lowest pressure, i.e. near the dry-wet transition line (salt zone, saturation line, Wilson line)[33]. At temperatures below the Wilson line, the build-up of deposit is less likely.

- Evaporation of condensates on hot surfaces

Evaporation of condensates mainly occurs in the wet steam region and in the “salt zone”, when the temperature of the metal surfaces is higher than the saturation temperature. On such a surface, all or part of the moisture evaporates and all non-volatile impurities are left. The turbine components surface can be increased above the saturation temperature by heat transfer through the metal from hot areas and by stagnant flow[33]. A typical area of LP turbine where evaporation of condensates may occur is the last row of discs, as explained earlier (Figure 5).

Figure 19 shows the deposition patterns compiled from analysis of samples from over 1000 turbines. It can be seen that most of the major impurities (chloride, sulphate, phosphate and sodium, etc.) are of the order of about 1%. However, these concentrations of impurities are measured as weight percentages of the deposits rather than the weight of impurities per area. Therefore, these data cannot be correlated to the impurity concentrations in the condensate.

Chloride of 0.03 mg/m^2 and 0.15 mg/m^2 would be left in the deposits on the turbine surface if the condensate containing 300 ppb and 1.5 ppm chloride were dried out, assuming that the thickness of the condensate layer were 100 μm. These values are significantly lower than those measured on deposits removed from blade surfaces, as shown in Table 10. In fact, 232 mg/m^2 would result in a chloride concentration of 2320 ppm (or 0.232%) in the condensate with a layer thickness of 100 μm. This

would suggest that the real contamination of impurities would be much higher than that calculated based on steady flow and under normal operating conditions. However, it is also possible that the deposits are accumulated during major chemical excursions. In addition, a build-up of deposits is also likely in the locations near the Wilson lines since these may move due to variation in the distribution of temperature and pressure in the turbines, resulting in local dry/wet steam cycles. These deposits may form some solid products and hence do not dissolve in the condensate.

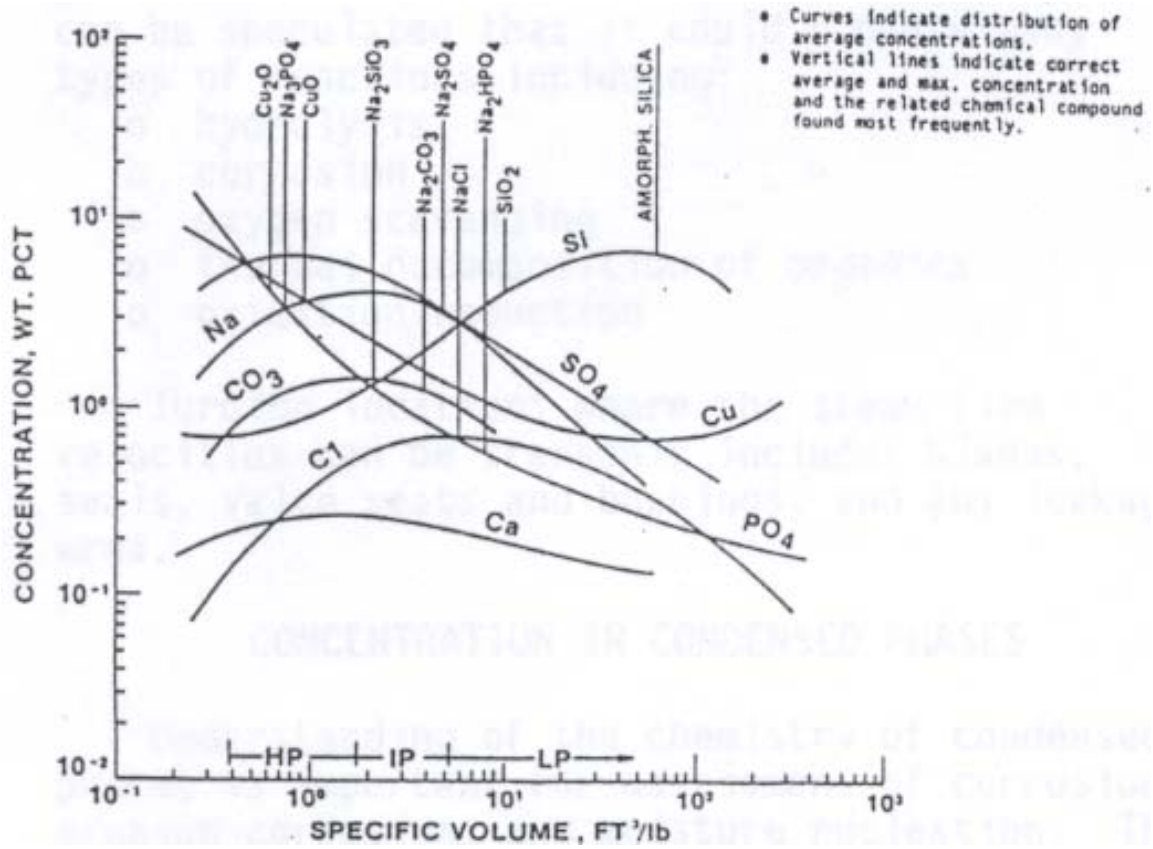

Figure 19. Deposition pattern found in Fossil Cycle turbines[33].

Table 10 Chemical analyses of deposits on blades failed from SCC[18].

Stage*	Cl^- (mg/m^2)		SO_4^{2-} (mg/m^2)	
	In	Out	In	Out
TA1	232	149	50	149
TA2	7.00	16.8	1.10	1.40

Note:
*** *Steam condensation occurs on both TA1 and TA2*
In: *Blade surface on the inlet steam side*
Out: *Blade surface on the outlet steam side*

Local chemistry in crevices

Crevices exist in the keyway region and where the blades are locked into the discs and will result inevitably in some change in local solution chemistry compared to that associated with the thin liquid layer on the steel surfaces external to the crevice. In principle, the crevice chemistry may be modified by evaporation or by electrochemical and chemical reaction, or indeed both. Evaporation-induced changes will result only when the steel is hotter than the steam. However, specific evidence of such changes in service is lacking and it is difficult to speculate on the significance as the range of possible chemistry modification is large.

A much clearer conceptual perspective exists in relation to reaction-determined crevice chemistry. On-load, the oxygen concentration in the external liquid film is negligible and there is no driving force for conventional crevice attack as commonly observed for stainless steels in seawater for example for which a large supporting cathode area external to the crevice is important to propagation. The electrode potential for the turbine steels will be low, and a lowering of the pH in the crevice is then very unlikely as the cathodic reduction of water within the crevice would be expected to oppose any tendency for a fall in pH. However, dissolution of MnS and retention of dissolution products in the crevice should result in the ready formation of pits and might be expected to encourage their early growth much more so than in an open deaerated system.

Off-load, when the liquid film is at equilibrium with oxygen in the atmosphere at about 3 ppm, the corrosion potential will increase, encouraging an increased corrosion rate in the crevice and ingress of chloride. The extent to which the pH will decrease is dependent on whether the crevice is formed between two disc steels or between a disc steel and a 12 Cr blade steel. In the former, the pH is not expected to fall below about 5 (pH value at temperature) and even here, this may not be attainable in the low conductivity solution associated with an off-load liquid film. The limitations in polarising the crevice off-load may be a factor limiting the fall in pH when the blade steel is present, despite the higher Cr level and larger hydrolysis constant for Cr. It would be surprising indeed if conventional crevice attack were to ensue. However, if the solution conductivity of the liquid film were to increase significantly off-load, the pH in a crevice containing the 12 Cr steel could fall to about 4 or less.

In fitting the blades into the disc rim, a lubricant MoS_2 is occasionally used. Predicting the crevice chemistry when this is present is not straightforward and emphasis should be on experimental measurement to assess its impact (see Section 2)

Conclusions

- Chemical control of the steam and water circuit

  The chemical control targets of boiler and feed-water depend on types of power plants and water treatments. The water chemistry in the once-through units is controlled more rigorously than that in the drum-type units.

  Under normal operating conditions, the cation conductivity of the condensed steam after cation exchange is controlled to less than 0.2 μS/cm. The oxygen

concentration in the steam is less than 5 ppb, except for oxygen treatment in which the oxygen is controlled to less than 50 ppb. The chloride and sulphate are controlled to less than 3 ppb.

- The temperature at which condensation occurs

  The distribution of steam temperature and pressure varies from station to station, depending on the turbine design and operating conditions. In the LP turbines, the temperature at which the first condensation occurs in UK power stations ranges from 70 °C to 120 °C. In the HP turbines, the first condensation occurs at a temperature above 250 °C in the PWR station and at approximately 170 °C in Magnox stations. Industry experience shows a link between the occurrence of disc cracking and the formation of condensates in the LP turbines.

- Chloride

  The chloride content in the liquid film is predicted to be 100 times higher than that in the steam, assuming that the liquid film commences to form at a moisture level of 1%. Therefore, the 300 ppb chloride concentration in the liquid film represents the upper limit under normal operating conditions, viz. when the chloride content in the steam is controlled to less than 3 ppb.

  1.5 ppm chloride concentration in the liquid film represents the upper limit if the chloride in the inlet steam is not monitored and controlled tightly, as 15 ppb Cl^- in the steam corresponds to a cation conductivity of the steam equivalent to 0.2 μS/cm, assuming chloride is the sole contaminant.

  Measurements at Moscow Electricity Institute indicate that the chloride concentration in the early condensate (as distinct from the liquid film) was about 10 to 50 times higher than that in the inlet steam. However, the chloride concentration in the liquid film was more variable, being 50 to 1000 times higher than that in the inlet steam. Evaporation was suggested as the possible cause for the presence of the much higher chloride concentration in the liquid films compared to that in the early condensates.

  A much higher chloride concentration was measured in the deposits. From chemical analysis of the deposit on the turbine surface, chloride level was found to be as high as 232 mg/m^2, equivalent to a concentration of chloride in the condensate of more than 2000 ppm, assuming the layer thickness were 100 μm.

- Other species

  Similarly, the predicted upper limit of sulphate in the liquid film is 300 ppb under normal operating conditions, if the sulphate content in the steam is controlled to less than 3 ppb. The maximum sulphate in the liquid film is 2 ppm if the sulphate in the inlet steam is not controlled tightly, as 20 ppb SO_4^{2-} in the steam corresponds to a cation conductivity of the steam equivalent to 0.2 μS/cm, assuming sulphate is the sole contaminant.

Organic species (total organic compounds) in the steam can be as high as 100 ppb. If all acetate ions were partitioned in the liquid phase, the maximum concentration of the acetate ion in the condensate would be 10 ppm. If the acetate ion at a concentration of 10 ppm were to form acetic acid, the pH of the condensate would be reduced to 4.3 at 90 °C. However, further work is needed to establish more reliably the concentration of acetate in the steam and the state of acetate compounds (acid or salts).

- Oxygen

  Due to the partitioning of oxygen between the steam and liquid phase, the oxygen in the liquid film and early condensate should always be less than 1 ppb under normal operating conditions.

  Under abnormal and transient conditions (air leakage, forced condensation, off-load), oxygen level of up to several ppms may be present in the condensates.

  Calculations based on the steady diffusion process show that oxygen dissolved in the condensation layer during the off-load period will be depleted quickly during start-up, assuming that the steam is oxygen free. For example, it only takes 8 seconds when the oxygen concentration on the metal surface reduces to 0.1% of the initial value, if the thickness of the condensation layer is 100 μm. However, it should be noted that the air leaked into the turbine chamber during off-load may take a long period to be removed completely. In-situ electrochemical measurements have revealed that the "corrosion activity" of steam turbine blades remains high for up to several hours depending on the type of the start-up.

- Carbon dioxide

  On-load, the carbon dioxide concentration in the liquid film is approximately 1 ppb when the inlet steam contains 1.5 ppm CO_2 (the estimated maximum CO_2 concentration due to leakage of CO_2 coolant in the reheater of an AGR power plant). Such a low level of CO_2 in the condensate would have no significant effect on the pH and conductivity of the liquid film.

  Similar to oxygen, the effect of CO_2 under transient conditions (e.g. off-load and start-up) may have a significant effect on the pH and conductivity of the condensates and hence EAC of turbine steels.

References

1. Model of Vaporous Carry-Over, Palo Alto, CA, Electric Power Research Institute, April 1981, NP-1787.
2. Deposition of Corrosive Salts from Steam, Palo Alto, CA, Electric Power Research Institute, April 1983, NP-3002.
3. Solubility of Corrosive Salts in Dry Steam, Palo Alto, CA, Electric Power Research Institute, June 1984, NP-3559.
4. Turbine Steam, Chemistry, and Corrosion, Palo Alto, CA, Electric Power Research Institute, August 1994, TR-103738.

5. Turbine Steam, Chemistry, and Corrosion, Experimental Turbine Tests, Palo Alto, CA, Electric Power Research Institute, September 1997, TR-108185.
6. Corrosion of Steam Turbine Blading and Discs in the Phase Transition Zone, Palo Alto, CA, Electric Power Research Institute, November 1998, TR-111340.
7. Modern Power Station Practice, Third Edition, Vol. C, Turbine, Generators and Associated Plant, British Electricity International, London, Pergmon Press, 1991.
8. Modern Power Station Practice, Third Edition, Vol. J, Nuclear Power Plant, British Electricity International, London, Pergmon Press, 1991.
9. G. Spink, Innogy, Private Communication, 2001.
10. Generation Operation Memoradum 72, CEGB, April 1983.
11. Cycle Chemistry for fossil Plants: All-Volatile Treatment, Palo Alto, CA, Electric Power Research Institute, April 1996, TR-105'041.
12. Cycle Chemistry for fossil Plants: Oxygenated Treatment, Palo Alto, CA, Electric Power Research Institute, December 1994, TR-102'285.
13. Cycle Chemistry for fossil Plants: Phosphate Treatment, Palo Alto, CA, Electric Power Research Institute, December 1994, TR-103'665.
14. Steam Turbines – Steam Purity, IEC, July 2000.
15. N. S. Cheruvu and B. B. Seth, Key Variables Affecting the Susceptibility of Shrunk-on Discs to Stress Corrosion Cracking, PWR-Vol. 21, The Steam Turbine Generator Today: Materials, Flow path and Design, Repair and Refurbishment, ASTM, p. 43-56, 1993.
16. F. F. Lyle, A. Mcminn and G. R. Leverant, Low Pressure Steam Turbine Disc Cracking – an Updata, Proc Instn Mech Engrs, Vol. 199, No. A1, p. 59 – 67, 1985.
17. D A Rosario, R. Viswanathan, C. H. Wells, G. J. R. Licina, Stress Corrosion Cracking of Steam Turbine Rotors", Corrosion, Vol. 54, No. 7, 531-545, (1998)
18. S. Maguire, BNFL, Private Communication, 2002.
19. D. Gass, Siemens, Private Communication, 2001.
20. Lyle, Jr. Paper No. 219, Corrosion/94.
21. D. W. James, Proc Instn Mech Engrs, Vol. 193, p. 531, 1979.
22. M. Brook, British Energy, Private Communication, 2002.
23. J. Ditchfield, BNFL, Private Communication, 2002.
24. O. Povarov, V. Semenov and A. Troitsky, Generation of Liquid Films and Corrosive Solutions on Blades and Discs of Turbine Stages, Specialist Workshop on Corrosion of Steam Turbine LP Blades and Discs, EPRI, February 9-11, 1998.
25. MTDATA, version 4.72, NPL, 1999.
26. Handbook of Chemistry and Physics, 74th Edition, CRC press, London, 1993-1994.
27. M. Nougaret, Alstom, Private Communication, 2001.
28. G. P. Quirk, British Energy, Private Communication, 2002.
29. G. J. Bignold and G. P. Quirk, Corrosion 2002, Paper No. 02333, 2002.
30. C. Bates, British Energy, Private Communication, 2002.
31. G. V. Vasilenko, Thermal Engineering, 38 (11), p. 51–54, 1991.
32. O. Jonas, Corrosion/77, Paper No. 124, 1977.
33. O. Jonas, Steam Chemistry and Turbine Corrosion – State of Knowledge, Proc. Int. Water Conf. Alto, CA, Vol. 54, p. 297-310, 1993.

Appendix

Analytic Solution to the Oxygen Diffusion Problem from Liquid Film

The governing equation for unsteady one-dimensional diffusion is (see Figure 13)

$$\frac{\partial c}{\partial t} = D\,\frac{\partial^2 c}{\partial x^2} \qquad 0 < x < l \tag{A.1}$$

where c is the species concentration, D the coefficient of diffusion (here assumed to be constant) and t and x denote time and distance measured within the slab of thickness *l*. Initially, we assume the concentration is constant throughout the slab, so

$$c = c_o \quad \text{when } t = 0\,. \tag{A.2}$$

The boundary conditions are

$$\frac{\partial c}{\partial x} = 0 \quad \text{on} \quad x = 0 \tag{A.3}$$

and

$$\frac{\partial c}{\partial x} + kc = 0 \quad on \;\; x = l\,. \tag{A.4}$$

where k is a rate constant and only the exchange with the steam phase is considered (reaction with the metal surface is ignored).

Condition (A.3) states that the species flux is zero on x = 0, and (A.4) that the flux is linearly dependent on the concentration on x = *l*.

The time dependence of oxygen concentration on the metal surface can be derived by solving Equation (13) with the above boundary conditions. Figure 20 shows the concentration of oxygen on the metal surface (x = 0) as a function of time at various values of ϕ ($\phi = kl$). It is clear when α is greater than 100, the oxygen depletion rate is independent of the value of α, i.e., the process is diffusion controlled. It also can be seen that the oxygen concentration on the metal surface is less than 0.1% of the initial value, c_0, when $\tau = 3$ ($\tau = tD/l^2$).

Therefore, it is readily possible to calculate the time, t, from the scaled time, τ, if the initial concentration of oxygen, c_0, the thickness of the condensate layer, *l*, and the diffusion coefficient of oxygen, D, are known.

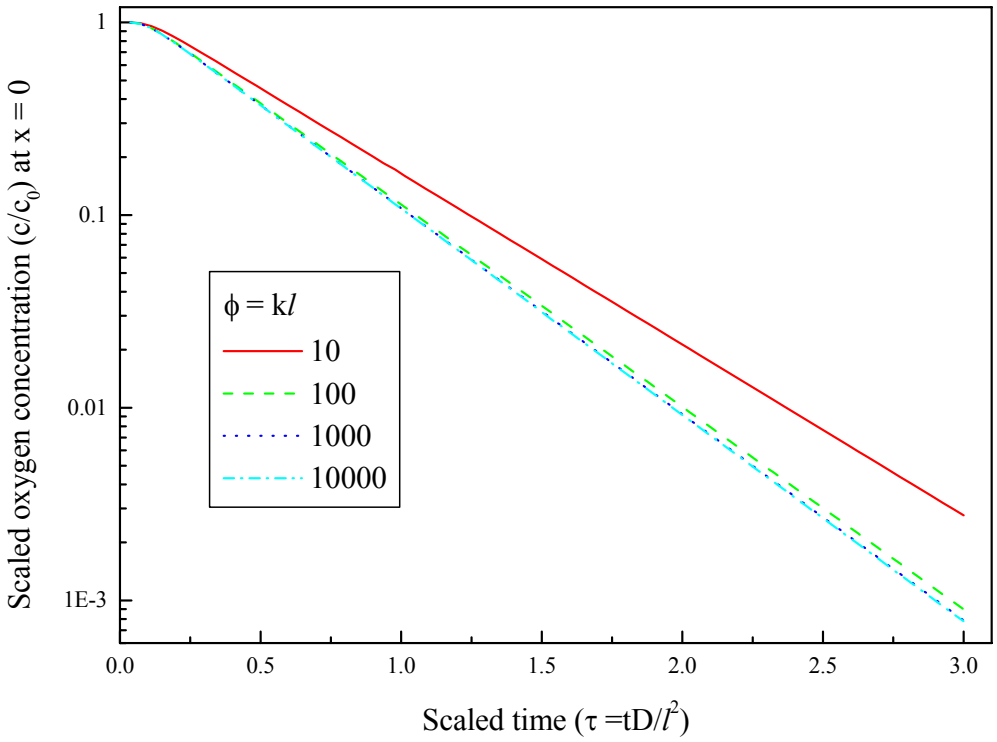

Figure. 20 Scaled oxygen concentration (c/c_0) on the metal surface (x = 0) as a function of scaled time (tD/l^2) at various values of α ($\alpha = kl$).

Nomenclature

AGR	Advanced Gas-cooled Reactor
CF	Corrosion Fatigue
EAC	Environment Assisted Cracking
EC	Early Condensate
HP	High Pressure
IP	Intermediate Pressure
LF	Liquid Film
LP	Low Pressure
PWR	Pressurised Water Reactor
PT	Phosphate Treatment
OT	Oxygen Treatment
SCC	Stress Corrosion Cracking

c	Concentration
K	Dissociation constant
K_w	Dissociation constant of water
l	Thickness of condensate layer
p	Partial pressure
y_n	Steam moisture or steam wetness
α	Conductivity coefficient
τ	Scaled time (t/Dl^2)
λ	Conductivity

SECTION 2 STRESS CORROSION CRACKING OF TURBINE STEELS

Cracking in Service

McMinn et al[1] reported that cracks on nuclear shrunk-on discs were found mainly at four locations: keyways, bores, web faces and rim attachment areas (Figure 1), with many of the failures initiated at some type of crevice (with crevice tightness a factor) and all were downstream of the location where the steam condenses in the turbine. Cracking was intergranular, along the prior austenite grain boundaries. Also, there was a strong relationship between cracking and the concentration of oxygen in the water-steam system of power plants.

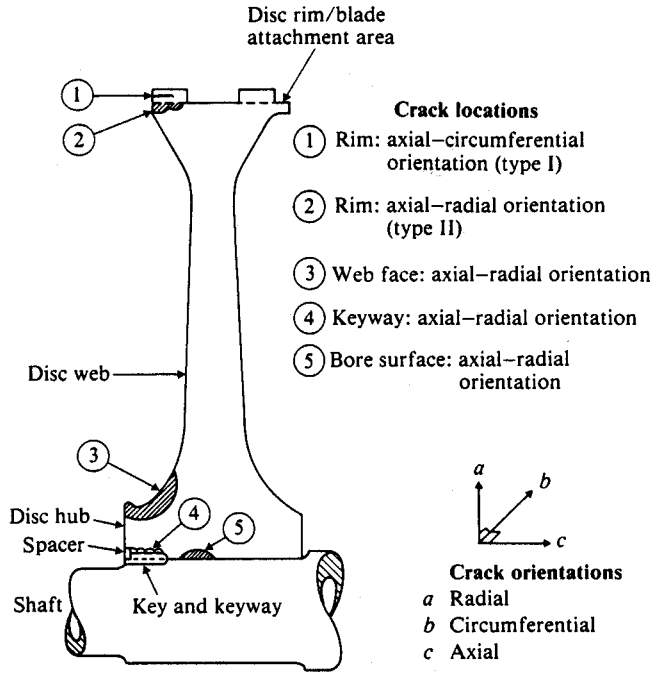

Figure 1. Locations and orientations of cracks found in low pressure turbine discs in US power plants (after McMinn et al[1]).

It is claimed[2] in a survey that nuclear power plants operating with air leakage below 4.7 litre/s have experienced no cracking incidents, whereas all those operating above 14.2 litres/s have exhibited cracking. Discs having either yield strength below 770 MPa or operating temperature below 104 °C experienced no significant cracking, as exemplified by Figure 2. Cracking was associated primarily with shrunk-on discs with little cracking of monoblock or welded rotors. In the latter case the most likely site of cracking will be the disc rim.

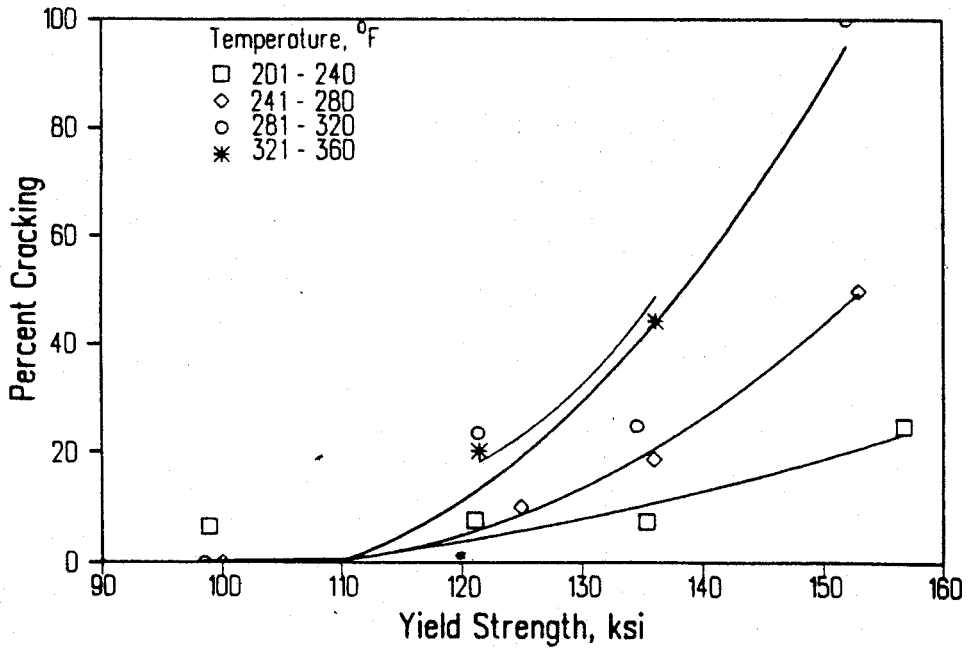

Figure 2. Incidence of cracking in service in relation to yield strength and temperature (after Sastry Cheruvu and Seth[2]).

In contrast with nuclear shrunk-on discs, where about 8% of all discs had experienced keyway/bore cracking, no cracking was observed on fossil reheat shrunk-on discs. Sastry Cheruvu and Seth[2] explain this on the basis that in general the dry/wet transition in a fossil reheat unit occurs at a lower temperature than in a nuclear unit. As a result more fossil discs operate in dry steam.

There are no reports of cracking in dry steam and it is argued that since the temperature in the wet steam region will be lower, the risk of cracking is very much reduced. However, they point out that the expansion line would be similar to that for the nuclear system for non-reheat machines or if NaOH were present.

Apparent crack growth rates in a nuclear turbine have been estimated[3] based on total operating times and observed crack depths and are represented in Figure 3.

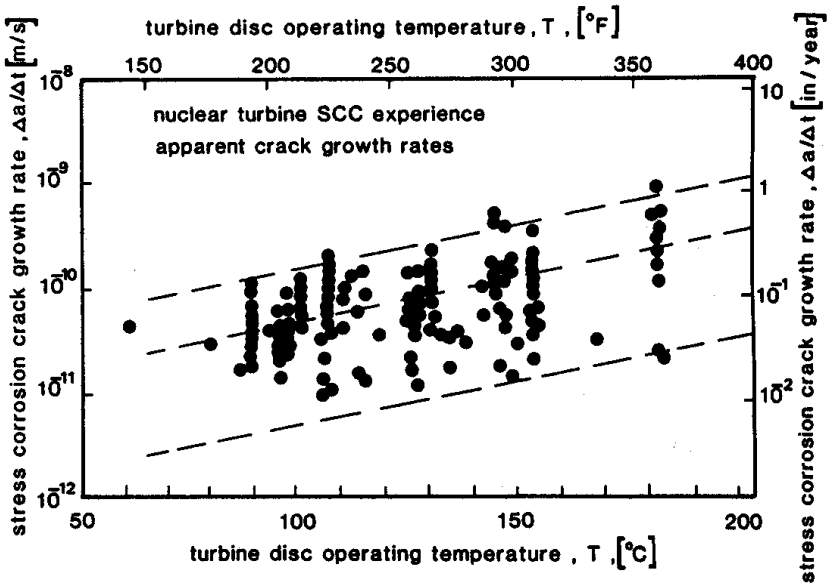

Figure 3. Crack growth rates estimated from service observations (after Speidel and Magdowski[3]).

These are claimed to be close to data from laboratory tests in aerated deionised water as shown in Figure 4.

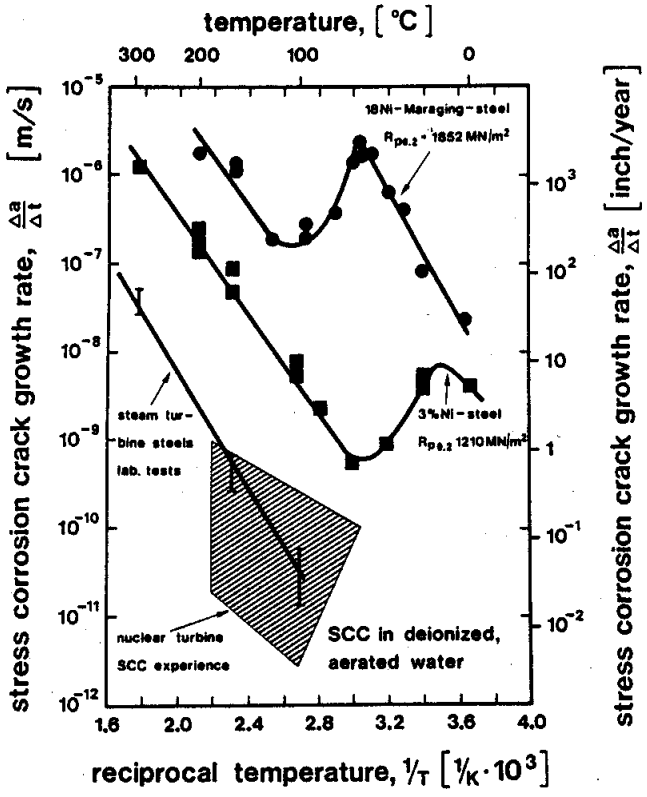

Figure 4. Crack growth dependence on temperature.

Lyons and Corish[4] carried out in-situ exposures of 12 Cr steel in a test chamber designed to receive a sample of steam from the bleed pipe supplying steam from the LP section of the turbine to the deaerator on a 45 MW single cylinder turbine. They noted that 200 ppb oxygen concentrations could be maintained for about 1000 h after a turbine cover lift and for a period of 24 h – 48 h due to infrequent minor air in-leakages.

Laboratory Testing

Disc steels

Stress corrosion cracking of turbine steel rotors has been reviewed in a number of papers, Rosario et al[5], Denk[6], Speidel et al[3,7,8]. The key features highlighted in those reviews will be presented and complementary information added as appropriate in order to benchmark the current position regarding laboratory test data and the effect of material composition, mechanical properties, stress state, environmental variables and their interaction.

Steel cleanliness

Viswanathan[9] has recently given a useful overview of the issue of steel cleanliness with respect to the properties of rotor steels. He summarises as follows. Impurity elements, viz. P, Sb, Sn, As, S, O, and deoxidants such as Al, Si can have a significant effect on the mechanical properties of steels. P, Sb, Sn and As interacting with Si and Mn can cause temper embrittlement leading to a reduction in K_{IC} and an increase in the ductile to brittle transition temperature (denoted FATT – fracture appearance transition temperature) whilst sulphide inclusions and non-metallic inclusions containing Al and Si can facilitate cavity nucleation at high temperature and ductile fractures in the upper shelf region giving reduced creep ductility at high temperatures and reduced K_{IC} at lower temperatures. Advances in processing have reduced impurity and deoxidant levels down to 20 ppm giving ‘clean’ steels whilst reduction of Mn, which is no longer required to ‘fix’ the sulphur, to 0.01% to 0.02% has resulted in ‘superclean’ steels. A superclean steel would contain approximately 0.001% S, 0.002% P, 0.02% Si, 0.02% Mn, which compares with a conventional disc steel of typically about 0.01% S, 0.07% P, 0.1-0.3% Si, 0.2% Mn.

The dependence of cracking on inclusion content of the steel is readily evident from the work of Holdsworth and Burnell[10], reproduced in Figure 5. Here, a microcrack is less than 250 μm in length (surface crack length). Similar results have been obtained by Endo et al[11].

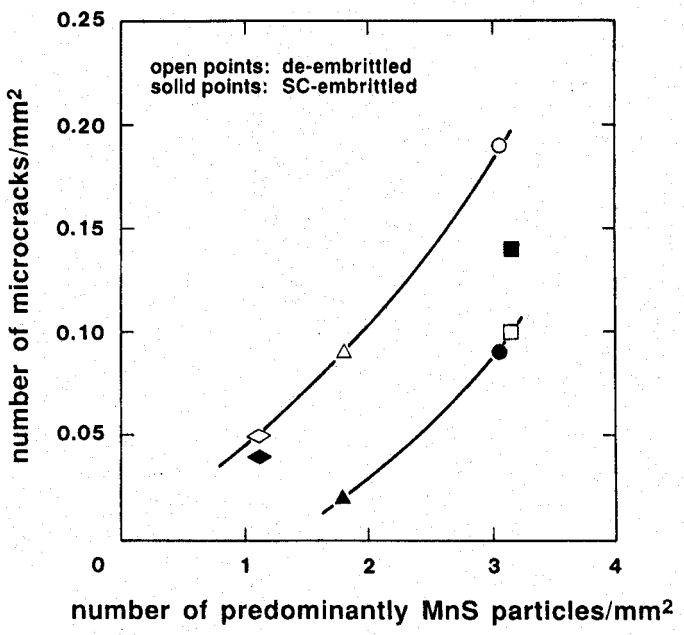

Figure 5. Relationship of microcrack density to inclusion density for medium strength disc steel (after Holdsworth and Burnell[10]). SC refers to stress corrosion.

The impact of superclean technology on stress corrosion cracking is not wholly clear in some respects. Rosario et al[5] suggest a marked improvement in life with respect to tests on plain specimens for which pitting corrosion (or perhaps localised straining at inclusions) acts as a precursor to cracking (Figure 6). However, crack growth rates were not affected (Figure 7).

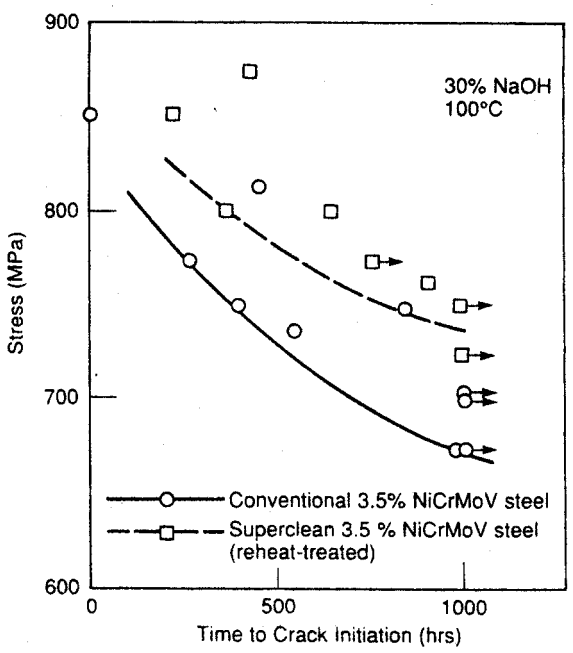

Figure 6. Comparison of time to cracking for conventional and superclean steels (after Rosario et al.[5]).

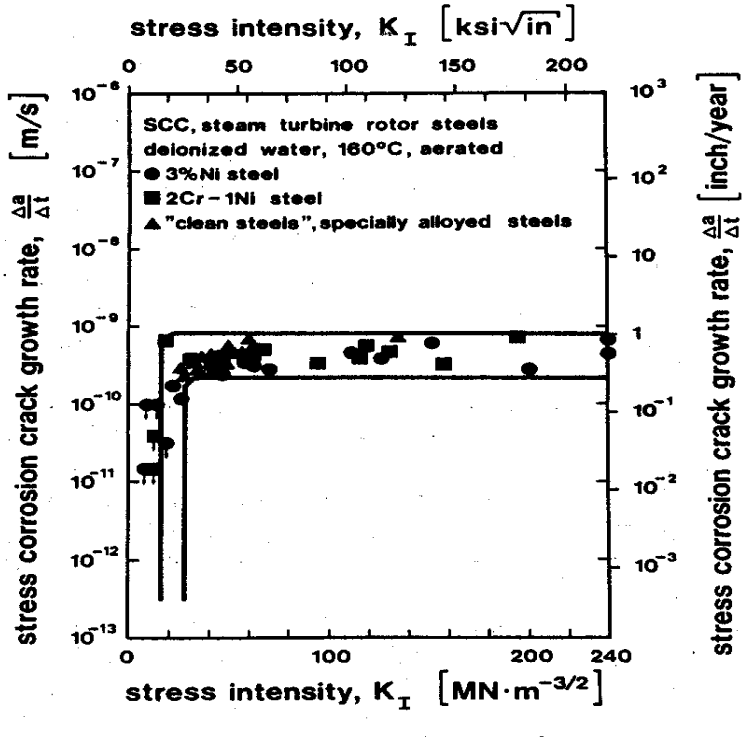

Figure 7. Crack growth in conventional and clean steels (after Speidel et al[3,7,8]).

The lack of dependence of crack growth rate on the stress intensity factor, suggested by Figure 7, might seemed to be queried by work of McIntyre et al[12] on 3.5 NiCrMoV steel. An increase in growth rate from 4.2×10^{-8} mm s^{-1} to 6.4×10^{-8} mm s^{-1} was reported when the K value was increased from 46 MPa $m^{0.5}$ to 69 MPa $m^{0.5}$. Tests were carried out in condensing steam at 95 °C but the extent of repeatability of the data was not indicated.

In contrast to some of the results above, Holdsworth and Burnell[10] reported measurements from various steels that suggested that P and residual elements at grain boundaries influenced long crack growth kinetics whilst having no effect on initiation.

Holdsworth and Thornton[13] investigated the effect of yield strength on cracking of conventional and superclean steels exposed to oxygen condensing steam at 95 °C (Figure 8). For medium strength steels (with $\sigma_{0.2} < 900$ MPa), microcracks (<250 μm) invariably nucleated from pits formed at surface breaking MnS inclusions and initiated after only 1000 h to 3000 h depending on strength level but took another 10,000 h to 30,000 h to develop to macrocracks (surface crack length of 1 mm). However, microcrack initiation in higher strength alloys was more likely from other surface breaking microstructural features. Also, there was less scatter in initiation and crack development times. However, it should be noted that all specimens were self-loaded to 100% of $\sigma_{0.2}$ and hence the actual applied stress on the higher strength steels is much greater. Of course there would be no point in using such materials unless taking advantage of their strength so testing near yield is important but it is useful to recognise that it may be the applied stress that is determining the low significance of pitting as a crack initiator. In relation to the medium strength steels, crack initiation did not occur with every pit and was not simply correlated with the deepest pit but

more with the mode of the distribution of pit sizes. Crack coalescence was more a factor with medium strength steels than high strength steels. The lines in Figure 8 indicate the lower and upper bounds for cracking of the conventional steels; the data points correspond to the two different superclean steels. When testing superclean medium strength steels, the time to microcracking was very much increased, whilst no evidence of macrocracking was observed after 50,000 h.

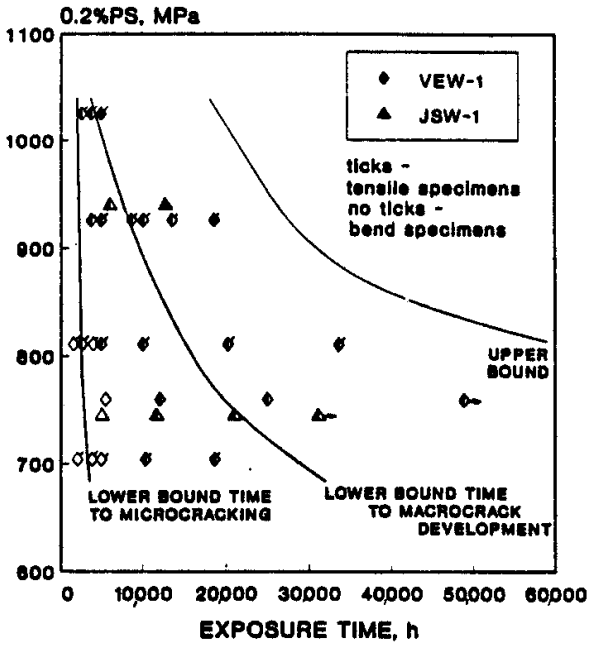

Figure 8. SCC crack development plot for two superclean medium strength 3.5 NiCrMoV rotor steel specimens loaded to their 0.2% proof stress in pure low oxygen steam at 95 °C. Open points correspond to no microcracking; part-filled points to microcracks; solid points to macrocracking and failure. Full lines relate to bounds for conventional steels (after Holdsworth and Thornton[13]).

For high strength steels, there was no benefit from steel cleanliness. Indeed, Holdsworth et al[14] reported an *inferior* resistance to SCC of superclean steel of 875 MPa strength level when tested at stresses close to yield in a condensing steam environment at 95 °C.

At strength levels of 700 MPa and 750 MPa, pitting and cracking of both superclean and conventional steel were observed by Denk[6] in stagnant aerated water with the conventional steel showing much higher density. In deaerated water, only the conventional steel showed pitting. It was suggested that stresses near the yield stress were required to form active pits. The development of pits at inclusions would be enhanced by the deformation of the interface, creating microcrevices and allowing pit development more readily. In 30% NaOH solution, intergranular cracks were observed at the same stress level in both steels with initiation attributed to a strain-controlled film rupture mechanism.

Gabetta and Caretta[15] measured pit density and growth rate for three 3.5 NiCrMoV steels in deionised deaerated water (<0.3μScm^{-1}) and in deionised water (probably partially deaerated but not well-defined) containing 100 ppb chloride, both at 80 °C. One steel was a superclean steel. Without chloride, pits nucleated from MnS inclusions in conventional steel and in a steel which had previously been used in service; the inclusions were dissolved after 5 hours. At about the same time period, for the conventional steel, inclusions containing Al, Si and other oxides were still undissolved but the interface between the inclusion and the matrix was heavily corroded. In the superclean steel, pit formation appeared to result from the corrosion of the steel matrix around inclusions, which are mainly small oxide particles. Not all such inclusions acted as initiation sites. Pit depth was a function of test duration but pit density was not.

After 200 h exposure, there was a higher density of shallow pits (< 25 μm) in the superclean steels than in the conventional steel but the number of deep pits was less. The 430 h specimens showed consistently a lower density of pits for all pit depths but maximum depths of about 160 μm were observed for the superclean steel compared with about 180 μm for the conventional steel. In parallel tests with an exposure time of 600 h, no pits were observed with a depth greater than about 130 μm whereas for the conventional steel, just less than 2/cm^2 were observed of depth 225 μm. The smaller number of shallow pits at long times compared with short times reflects a reduced tendency for nucleation with time.

The authors indicate that the pit growth rate was also higher in the chloride-containing solution when compared to the chloride-free solution. However, the extent of aeration of the chloride-containing solution was not established.

As noted below in the section on Creviced Specimens, Lyle[16] tested a 740 MPa yield strength disc steel in water of three different purity levels at 130 °C under simulated crevice conditions. The time to initiate cracks in the superclean steel was about 70% of that for the conventional steel and the cracks were deeper. Cracks initiated in grain boundary trenches rather than at pits.

It would appear that there is not complete consistency with respect to the effect of steel cleanliness, which appears to be strength level and stress level sensitive. It is claimed that there is a lack of an effect of cleanliness on long crack growth, although there are apparent exceptions, and it is unclear whether there is any impact on short crack growth.

Strength and temperature effects

Strength level and temperature are considered the two dominant parameters in relation to stress corrosion cracking of disc steels. In relation to the rate of propagation of cracks, Speidel et al[3,7,8] suggest a weak dependence on strength level at values between 600 MPa and 1100 MPa with a greater sensitivity above 1100 MPa (Figure 9) which he attributed to a change in cracking mechanism to hydrogen embrittlement. Further support for this hypothesis is given by the temperature dependence of the crack growth rate for the higher strength alloys, as shown in Figure 10, the peak in growth rate being often characteristic of a hydrogen

embrittlement mechanism. Deaeration in these tests was with argon, with no apparent measurement of the oxygen concentration.

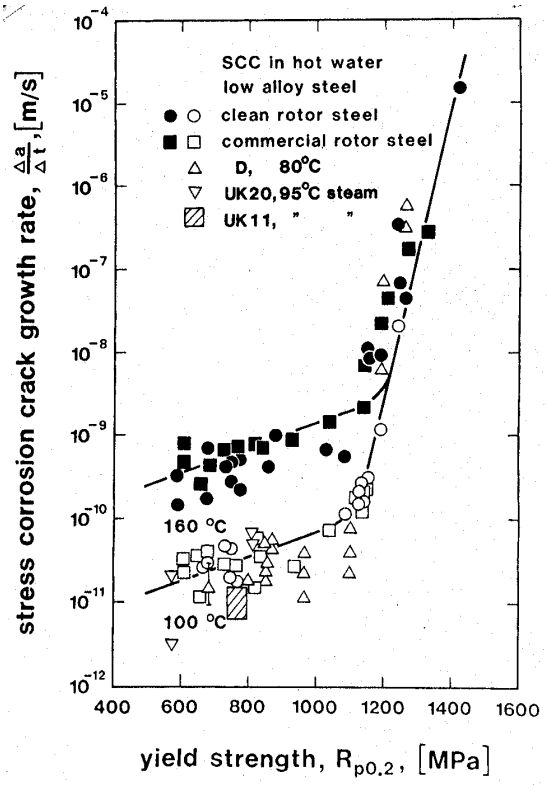

Figure 9. Growth rate dependence on yield strength for 3.5 NiCrMoV disc steel (after Speidel[3,7,8]).

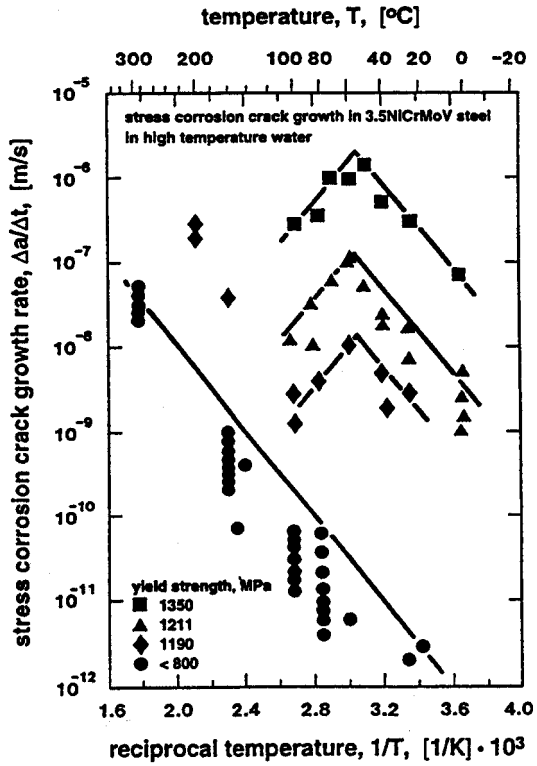

Figure 10. Growth rates of intergranular cracks in 3.5 NiCrMoV rotor steel. (after Magdowski and M.O.Speidel[3]).

The impact of strength level and temperature is well represented by growth rate equations as summarised by Rosario et al[5]. From Clark[17]:

$$\ln R = -9.922 - 4053/T + 4.03 \times 10^{-3} \sigma_{ys}$$

Subsequently, this was updated to:

$$\ln R = -13.75 - 2242.4/T + 3.35 \times 10^{-3} \sigma_{ys}$$

Further analysis allowed for the effect of Mn. For materials tempered above 566 °C (1050 °F):

$$\ln R = -9.69 - 5145.3/T + 0.0337 \sigma_{ys} + 4.53 Mn$$

The original units have been converted in the above such that R is now derived as mm s^{-1}, T is in degree Kelvin, σ_{ys} is in units of MPa and Mn is in mass%.

The authors provide an expression for the effect of Mn and for a tempering temperature below 566 °C but substitution of the tempering temperature into the equation as defined gives unreasonable results and suggests an error in the presentation. Accordingly, this equation is not reproduced.

In relation to testing of plain or crevice specimens with no pre-existing cracks or defects, the perception of the influence of strength level would seem to depend strongly on the environmental exposure conditions. Sastry Cheruvu and Seth[2] reported no significant cracking below 758 MPa, based on field experience. However, in creviced stress corrosion cracking tests at 130 °C, Lyle[16] showed that cracking does occur at the lower strength levels in the presence of oxygen at 40 ppb level with 20 ppb chloride, but not pure water with 5 ppb oxygen. Nevertheless, the higher strength alloys (about 940 MPa) cracked in the latter environment and cracks were deeper in the oxygen-containing environments.

Lyle and his co-workers[18] infer that there is no effect of yield strength on SCC susceptibility on the basis that turbine discs that had cracked in service had widely varying yield strengths. However, they did recognise an effect on growth rates.

Holdsworth et al[19] investigated the impact of strength level on cracking as shown in Figure 11. Clearly, increasing the strength level reduces the time to macrocrack formation. Nevertheless, it would have been of interest to have conducted tests at the same stress level on the different steels to assess the intrinsic effect of material property change.

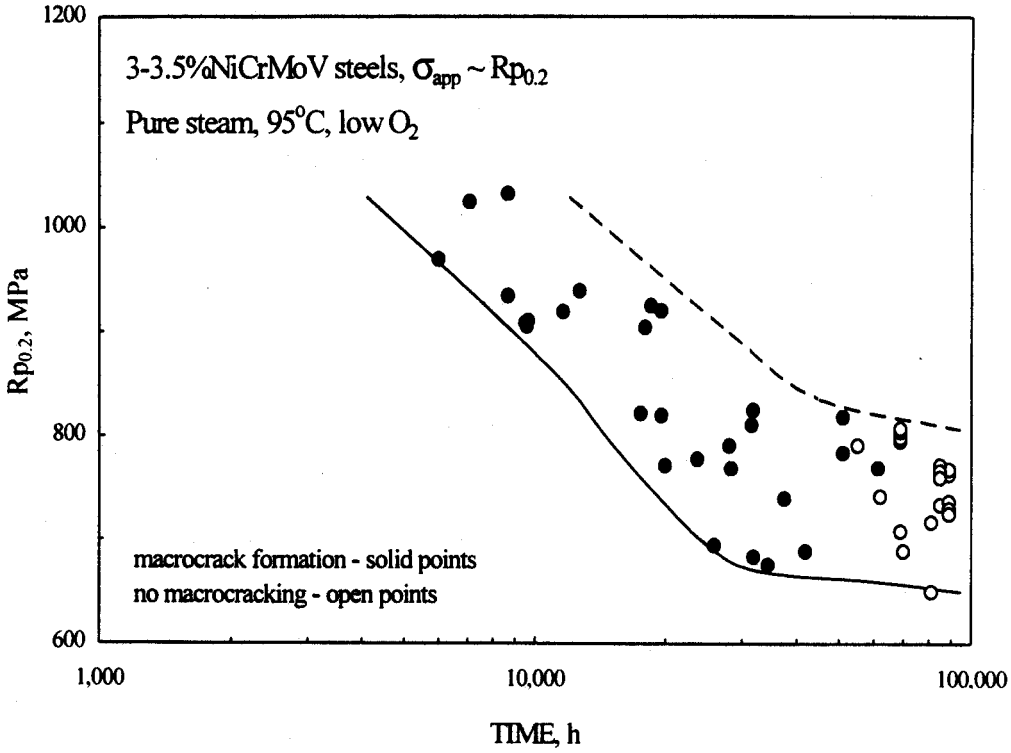

Figure 11. Effect of strength on the time to macrocrack formation in pure condensing steam (after Holdsworth et al[19]).

Environmental variables

Speidel et al[3,7,8] have summarised the effect on cracking of a number of environmental variables. The effect of oxygen concentration on the corrosion potential and the cracking mode is shown in Figure 12. There is no indication as to whether the corrosion potential had attained its steady value prior to failure but increasing potential does cause a progressive change from ductile to intergranular to transgranular failure with the area associated with SCC also increasing. Carbon dioxide increased the proportion of intergranular failure.

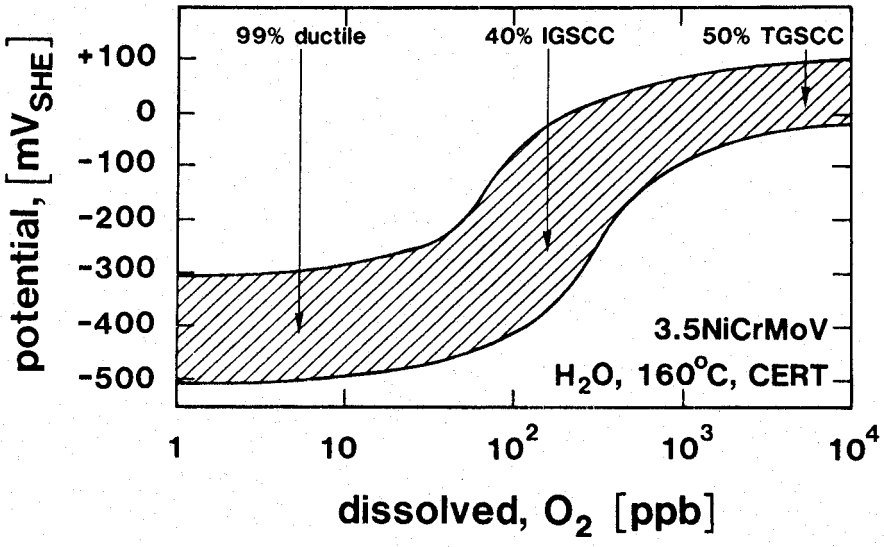

Figure 12. Effect of oxygen concentration on potential and fracture mode in constant extension rate tests (after Speidel et al[3,7,8]).

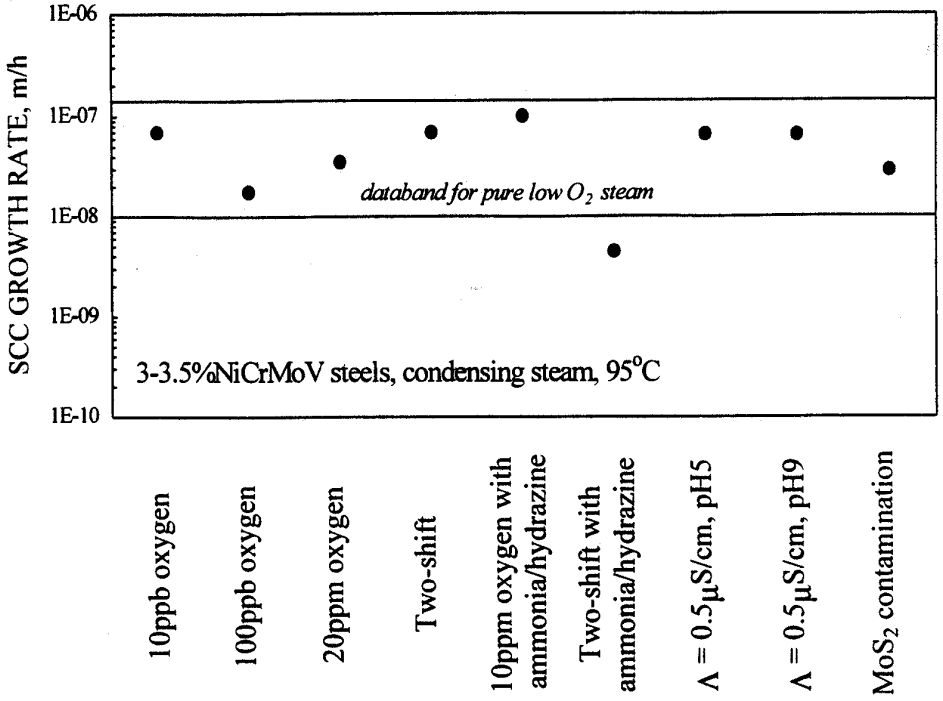

Figure 13. Influence of environment composition on plateau crack growth rates from WOL (Wedge-Opening-Loading) testing of disc steel in condensing steam (after Holdsworth et al[19]).

Holdsworth et al[19] conducted crack growth studies using WOL specimens and showed little impact of feedwater oxygen level up to 20 ppm (Figure 13) Adoption of a two-shift simulation in terms of environment cycling from condensing steam at 95 °C for 16 h to exposure to trickling of de-ionised deoxygenated water into the aerated test

vessel for 8 h at 70 °C gave similar results within the scatter band established for pure condensing steam under nominally constant conditions. The use of an ammonia/hydrazine treatment gave a discernible improvement in combination with the two-shifting environment but not in condensing steam on its own. Increasing the conductivity (by addition of Na_2SO_4 into the steam line as a fine droplet spray after the boiler) or pH had no impact on crack growth in condensing steam, whilst MoS_2 lubricant contamination also had no effect, the rational being that in the WOL test the lubricant was confined to the notch and had no impact on crack tip chemistry. This is in contrast to the behaviour for plain specimens where a dramatic effect of MoS_2 is observed (Figure 14). Here also a clear effect of solution conductivity can be discerned, whilst for the same conductivity pH does not seem to have an effect.

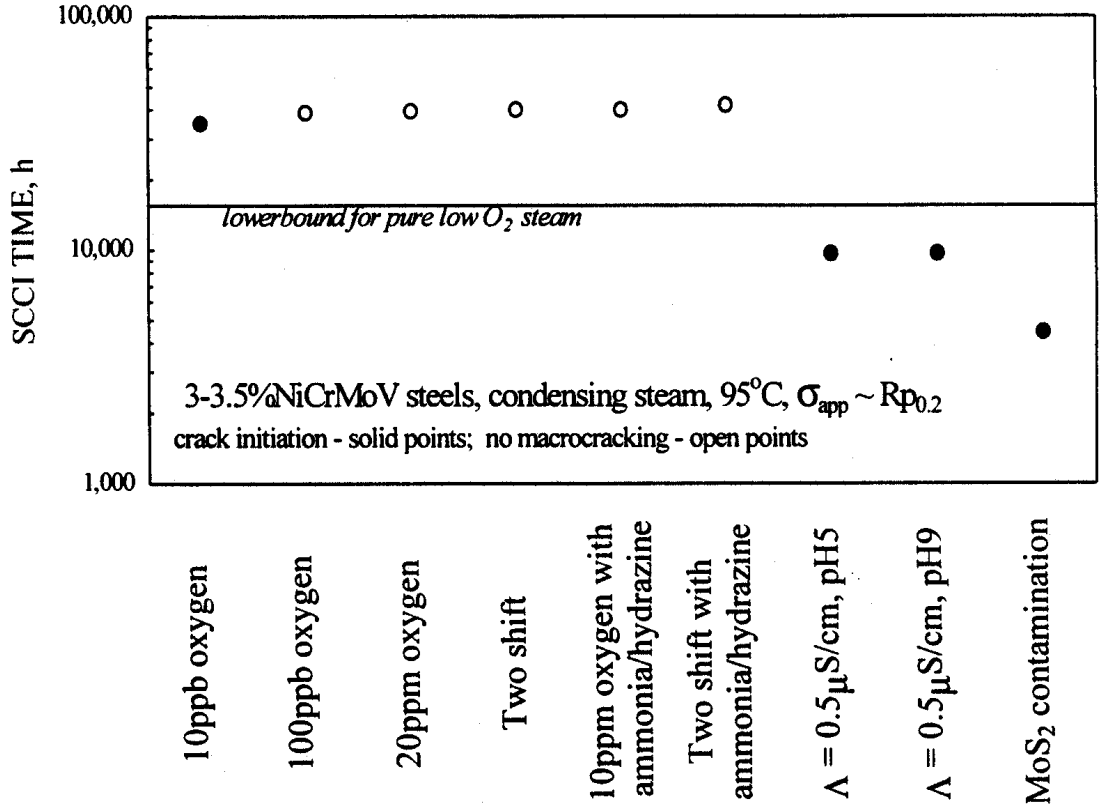

Figure 14. Influence of environment composition on time to macrocrack initiation in disc steel in condensing steam (after Holdsworth et al[19]).

In testing by Kondo et al[20] on 3.5% NiCrMoV steels, an increase in solution conductivity decreased the number of cycles to crack initiation (defined at a crack depth of 0.5 mm), Figure 15, but had no impact on the crack propagation rate (Figure 16), in this 100 ppb oxygenated solution at 60 °C, consistent with the observations of Holdsworth et al[19].

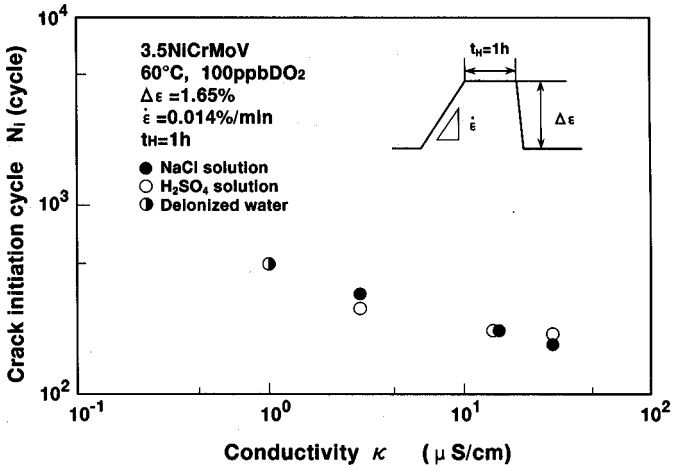

Figure 15. Impact of solution conductivity on number of cycles to crack initiation (after Kondo et al[20]).

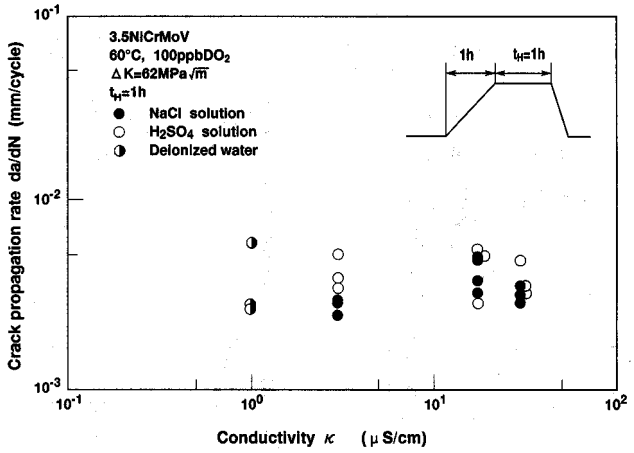

Figure 16. Impact of solution conductivity on crack growth kinetics (after Kondo et al[20]).

However, the critical role of pH, or more precisely dissolved CO_2, was highlighted by Schleithoff[21] in rationalising the observation of disc cracking in South Africa but none in Europe for the same system, the main difference being the power plant water chemistry system; more free acids being noted in the South Africa unit condensate. Scheithoff considered that CO_2 in the steam was the key factor. The impact of CO_2 is clearly observed in the laboratory results of Figure 17. However, the precise concentration of CO_2 in the testing was not defined.

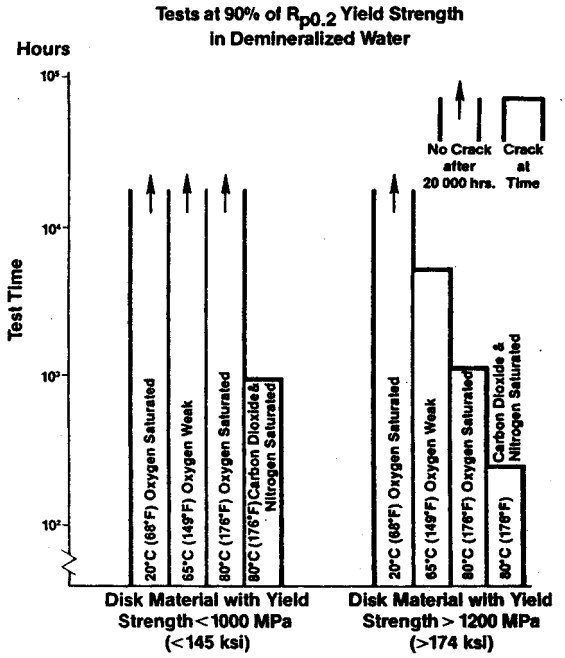

Figure 17. Stress corrosion test results (after Schleithoff[21]).

In contrast to the results of Schleithoff, which may reflect the influence of dissolved gases on pitting and early crack development, long crack growth rates measured by Speidel et al[3,7,8] showed no discernible dependence on oxygen concentration or on CO_2 level as shown by Figures 18 and 19.

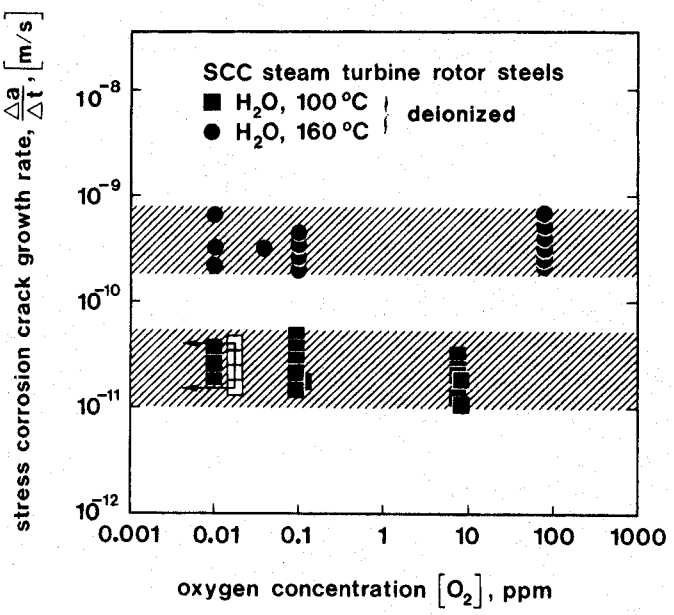

Figure 18. Effect of oxygen on stress corrosion crack growth kinetics of rotor disc steel (after Speidel et al[3,7,8]).

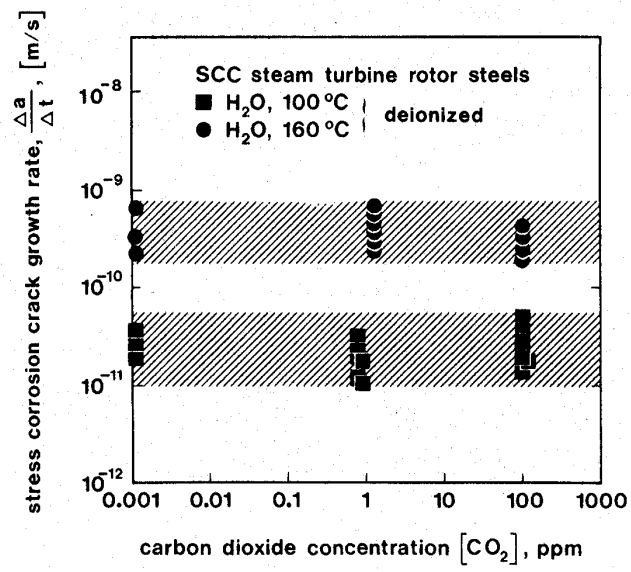

Figure 19. Effect of CO_2 on stress corrosion crack growth kinetics of rotor disc steel (after Speidel et al[3,7,8]).

Speidel et al suggest that whilst pitting was significant in condensing steam, measurements in a closed autoclave system under fully immersed conditions, aerated and deaerated, gave no indication of pit growth despite an increasing conductivity with exposure time. They concluded that water as a bulk environment is less aggressive than condensing steam although the content of impurities might be higher than those of the feed-water of the steam cycle. The details of the tests are not given in the review by Speidel et al, but current experience at NPL[22] shows that pitting of self-loaded tensile specimens stressed to 90% of the 0.2% proof strength does occur in refreshed aerated and deaerated pure water at 90 °C, with depths of about 100 μm after a year. In aerated solution with 1.5 ppm chloride the pit density and growth rate were significantly greater.

In contrast to the observations at NPL, David et al.[23] reported no pitting in both high purity (<0.2 μScm^{-1}) deaerated water and in oxygen-saturated water even for 25 year-old conventionally smelted steel, for which the MnS inclusion density would be significant. Further, no cracking was observed in aerated or deaerated pure water unless the strength level was greater than about 1000 MPa as shown in Figure 20. At the lower strength levels, testing was extended to almost 3.4 years. From their own observations and that of others they provided a crude guideline for the incidence of cracking as shown in Figure 21. The less "aggressive" the environment, the higher the operational stresses, relative to the proof strength, that can be tolerated. However, as indicated in Section 1, high purity water is not the relevant environment to describe the liquid film formed on turbine discs on load because of the partitioning of chloride, sulphates etc. from the steam phase to the liquid phase.

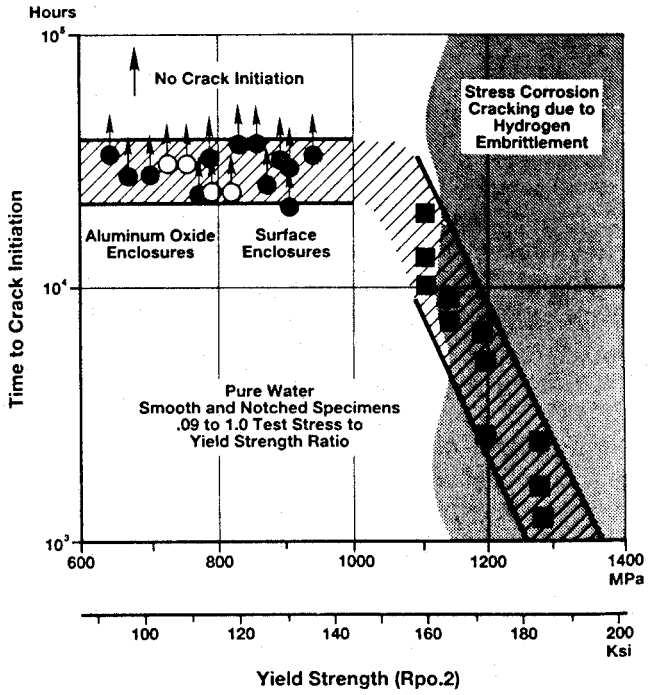

Figure 20. Crack initiation testing on LP turbine rotor and disk materials[23].

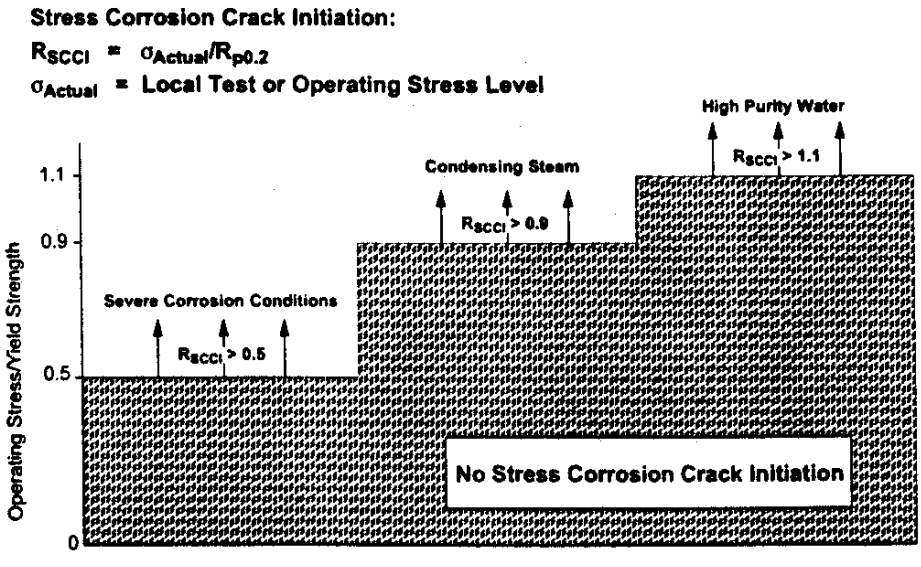

Figure 21. Stress corrosion crack initiation of LP turbine rotor and disc materials[23].

Sparkes et al[24] argued that pitting corrosion in a turbine was predominant at 75 °C under off-load conditions; the maximum pit depth could then be related to the number of cold starts (N) experienced by the shaft:

$$d_{max} = KN^{n}$$

where K is a constant, sensitive to the station details, and n is the exponent in the pit growth law.

Many of the tests conducted by McMinn et al[1] and by Speidel et al[7,8] have been at a temperature close to 160 °C, which the former authors claim is a representative temperature at which disc cracking has been found in nuclear LP turbines in the USA. The results from self-loaded WOL tests by McMinn et al are shown in Table 1 and Figure 22.

Table 1 Maximum crack growth rates obtained from bolt-loaded WOL specimens.

Material	Yield Strength MPa	Crack Growth Rate, mm/year: Deaerated 10% NaOH	Oxygenated 10% NaOH	Deaerated 1% NaOH + 0.1% NaCl	Aerated 1% NaOH + 0.1% NaCl	Deaerated Pure Water	Aerated[3] Pure Water	Carbonated[3] Pure Water		Oxygenated[3] Pure Water	Field Data at 157 C[11]
N	1124	1182	259	79	53	23	197	70[4]	14	3.2	11.6
E	876	334	32	4.4	0.5	4.5	16	1.7[4]	14	11	4.3
U[1]	821	123	14	3.6	0	3.6	8.1	2.5[4]	26	0	3.4
O	731	244	68	5.8	3.1	1.1	4.6	3.0[4]	7.2	0.9	2.4
OH[2]	717	203	78	3.1	5.8	4.1	20	—	7.2	4.5	2.3
ZZ	706	7.4	—	—	—	4.2	—	3.8[4]	—	—	2.1
VV	627	8.9									
Steay-State Electrode Potential, mV (SHE)		−670 to −780	+30 to −210	−700 to −760	+170 to +120	[5]	+30 to −200	+250 to +130		+290 to +235	

[1]Electroslag remelted.
[2]Temper embrittled 1000 hours at 480 C (896 F).
[3]A single set of specimens was used for tests in aerated deionized water, carbonated deionized water, and oxygenated deionized water. Specimens were exposed to the three environments in the order indicated.
[4]Virgin specimens.
[5]Not measured.

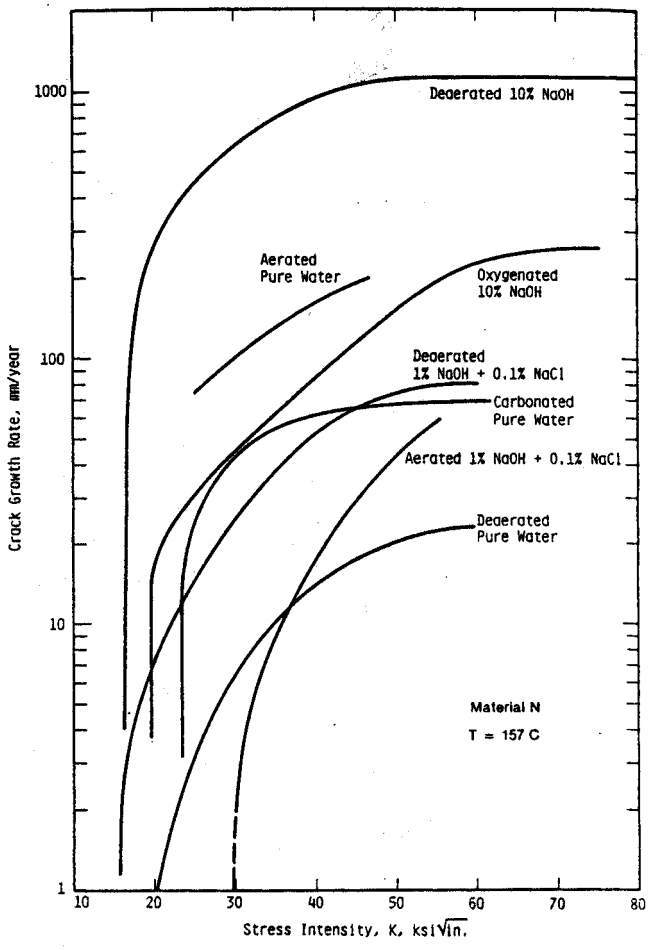

Figure 22. Impact of environmental variables on stress corrosion crack growth kinetics (after McMinn et al[1]).

For the aerated, carbonated and oxygenated environments a 10 psi (0.07 MPa) overpressure was maintained. The electrode potential was also monitored and is included in Table 1. The high values associated with oxygenated and carbonated solutions relative to aerated solution should be noted. McMinn et al make the following observations. Yield strength has a dominating effect. They note also that P segregation to gain boundaries accelerated crack growth rates in dilute solutions, although yield strength is far more significant. Cracking was transgranular in aerated water but intergranular in carbonated and oxygenated water. They refer to the observations of Hodge and Mogford[25] that cracking in UK turbines was predominantly intergranular but the initial portions were usually transgranular. They report other work by McMinn et al on crack initiation studies that indicate that crack initiation was transgranular and that air additions accelerated the initiation process. High CO_2 levels accelerate cracking with respect to oxygenated environment although not with respect to aerated solutions (Table 1). The authors did not provide a mechanistic rationale for the observations.

They suggest also that since growth rates estimated from service agree with those from laboratory tests for deaerated dilute environments it can be assumed that concentrated NaOH solutions are not responsible for cracking and that whilst aeration has an effect on initiation it does not have an effect on propagation, despite the laboratory results noted above in Figure 20.

Holdsworth and Burnell[10] reported that SCC initiation tests using self-stressed bent-beam specimens indicated no macrocracking (surface breaking crack of length 1 mm) after 22000 h in pure low-oxygen condensing steam (feedwater: 0.1 μScm^{-1}) at 95 °C and in a cyclic steam environment (16 h pure steam at 95 °C, 8 h humid air at 70 °C). The specimens were loaded up to varying stress levels with a maximum of 110% of the 0.2 % proof strength. However, pits to a depth of 50 μm and microcracking from the tensile side of the specimen were observed at times between 2000 h and 5000h. The authors do not distinguish the impact of the exposure conditions on the pitting and microcracking observed.

Creviced specimens

Lyle[16] studied the initiation of stress corrosion cracking in three 3.5NiCrMoV steels with a range of Mn and S including a high purity material. The environments were:

- high purity water ($<0.3\mu S^{-1}$) with 5 ppb oxygen;
- 20 ppb NaCl solution containing 40 ppb oxygen;
- contaminated solution, i.e. 20 ppb NaCl with air saturation (6-8 ppb oxygen).

Tests with creviced and uncreviced specimens were conducted at 130 °C, the temperature of the Wilson line where water first condenses in some turbine designs. The specimens were either 3-pt bend loaded to 70% or 90% of yield or in the form of U-bends.

In the contaminated solution, cracks initiated from trenches or at phase boundaries and were intergranular. A few instances of cracks from pits were observed. Cracking in the 3-pt bend tests was confined to crevice specimens. For the intermediate oxygen level (40 ppb with 20 ppb NaCl), the behaviour was fairly similar to that for the

contaminated solution. In the low oxygen high purity water, cracks took much longer to initiate but otherwise were similar to the other environments. Cracks were deeper for the same time period in the higher stressed specimens in all cases. The cracks in all cases were found mainly along the edges of the tension-loaded surfaces of the creviced specimens in localised etched zones. Corrosion product shielding of oxygen supply to the crevice was considered to be the key factor in generating crevice corrosion, with the conventional differential aeration cell mechanism being operative. However, this is not a tenable explanation for the 5 ppb oxygen test. It was also concluded that the number and type of inclusion was not a factor. Notably the high purity steel, with low Mn and S, exhibited deeper cracks in most cases compared with the conventional steel of the same yield strength. Cracking in all cases, including the high purity alloy, was intergranular.

Clearly, the presence of crevices adjacent to the stressed surface increases the likelihood of cracking (see Discussion section).

Surface state

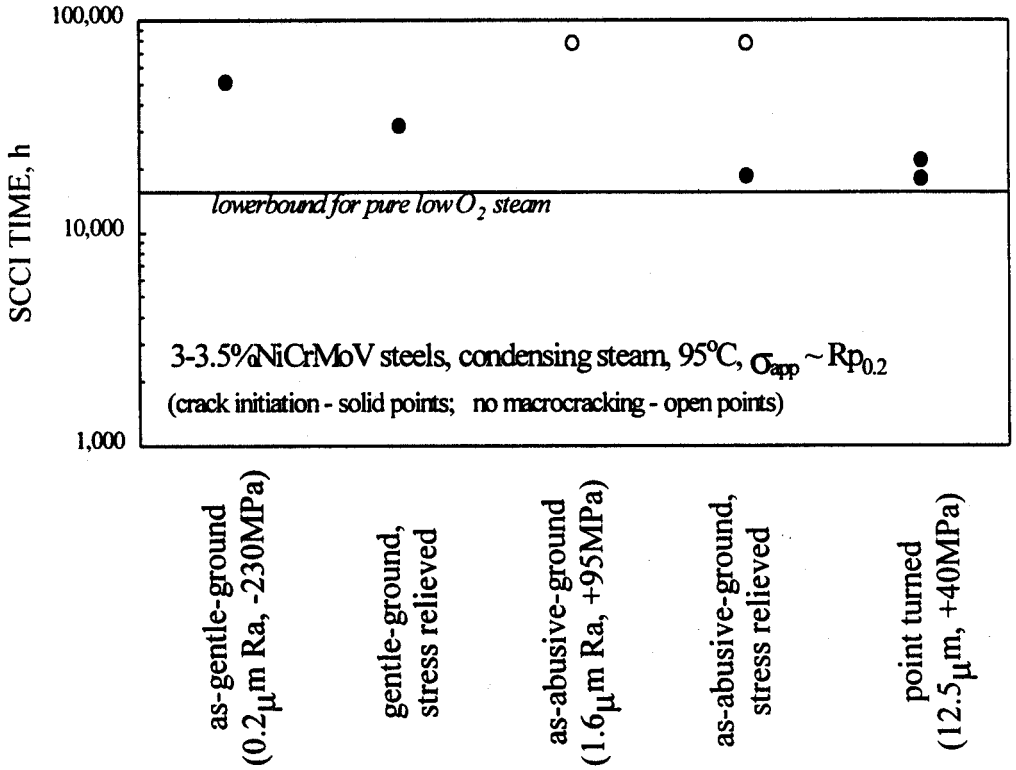

Figure 23. Influence of surface condition on the time to macrocrack formation for a medium strength steel in condensing steam at 95 °C (after Holdsworth et al[19]).

The effect of different methods of grinding the surface was explored[19], as both surface roughness and residual stresses are influenced and could affect crack initiation (Figure 23). There is a tendency for rougher surfaces to lead to shorter crack initiation times but within the overall databand established with the standard specimen with the same controlled finish. The effect of residual stress from grinding was more variable

and this was attributed to the influence of pitting which could proceed beyond the affected depth. This study would have been of more value for the high strength steel where surface features can have more significance.

Corrosion fatigue/Two-shifting

The results of corrosion fatigue tests of a disc steel using plain or pre-pitted specimens are shown in Figure 24 (after Speidel et al[7,8]). The reference data were obtained in air at ambient temperature rather than test temperature and this makes comparison of results at different temperatures uncertain. At lower temperatures there would appear to be an effect of dissolved CO_2 as aerated water, containing dissolved CO_2 from the atmosphere, was more aggressive than oxygenated water. This may have been a factor also in the pre-pitting tests although the latter would clearly be affected simply by exposure time. There was no reference to the cyclic frequency but the high number of cycles indicates that this would have been high so that the environmental effect on life may have been confined mainly to the impact on pitting as a stress concentrator. In such circumstances, test time becomes important as the pit depth would continue to increase with time. This may explain the surprising lack of effect on relative fatigue life of deaerated water. It is known that pitting and deep pits of 100 μm can be obtained but the growth rate is low. Thus, the data in Figure 24 should be considered as indicating simply relative aggressivity of the exposure conditions.

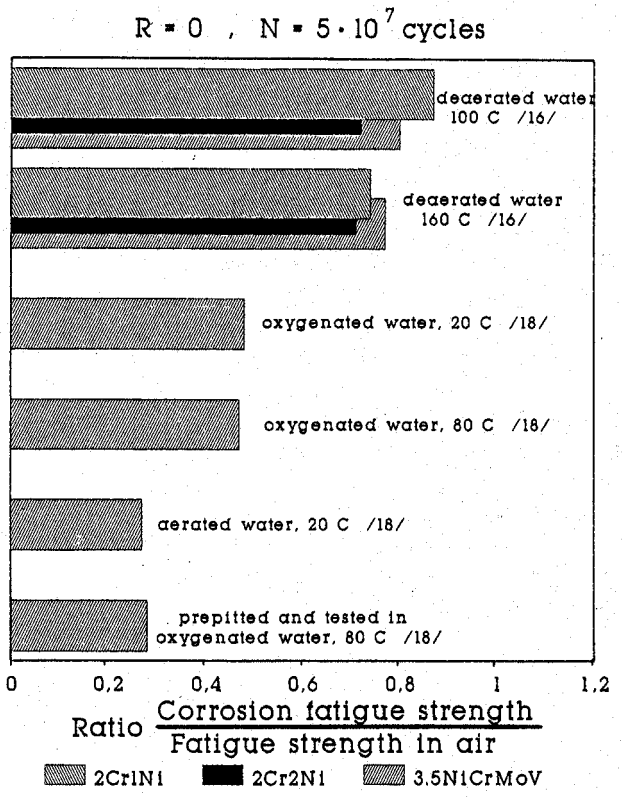

Figure 24. Impact of environmental variables on the corrosion fatigue strength of disc steels (after Speidel[7,8]). The numbers in the figure refer to references in the cited paper.

The results of further tests following pre-corrosion are shown in Figure 25. The notch effect of pitting is more apparent but as noted above, the test may have been too short to observe an effect of pitting in the deaerated water.

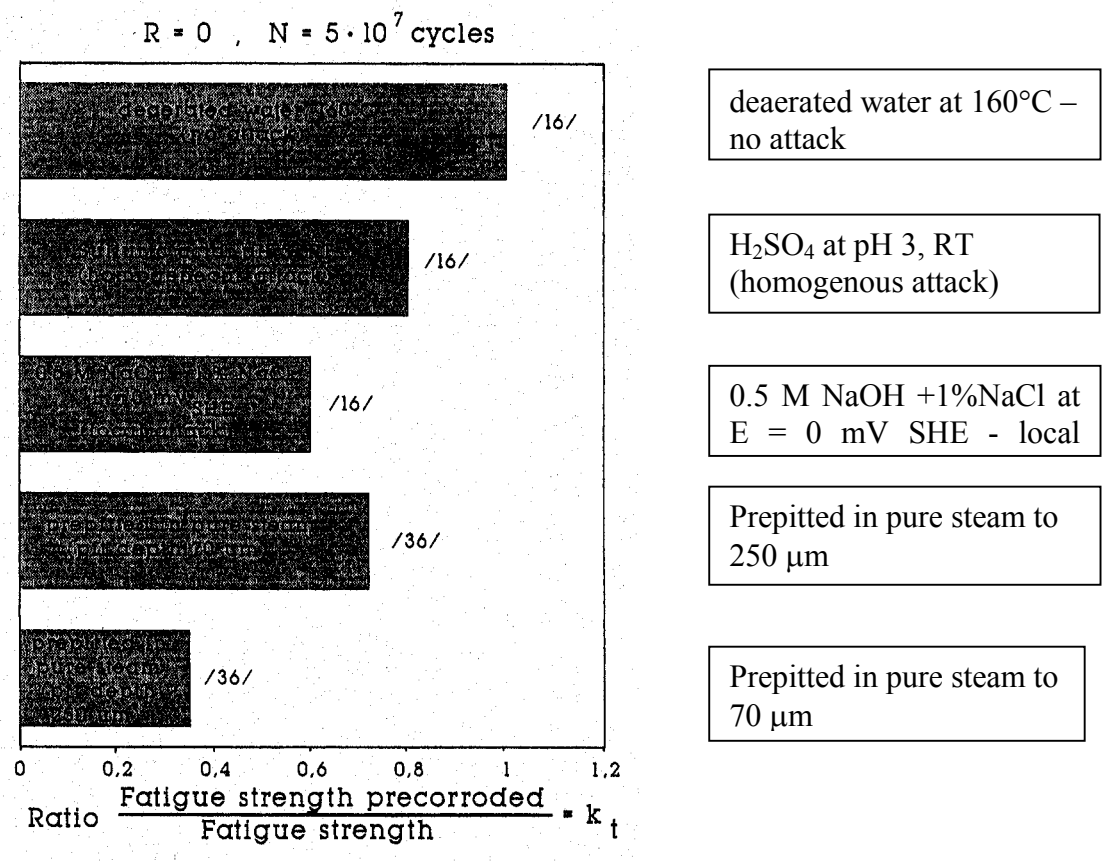

Figure 25. Impact of environmental variables and pre-exposure on the corrosion fatigue strength of disc steels (after Speidel[7,8]). The numbers in the figure refer to references in the cited paper.

Crack propagation measurements were carried out as part of the same programme and suggest an increase in crack growth rate, relative to air data, in the aqueous environment at 100 °C down to very low ΔK values as shown in Figure 26.

In the review quoting this work the cyclic loading frequency was not defined and the original references were not readily accessible.

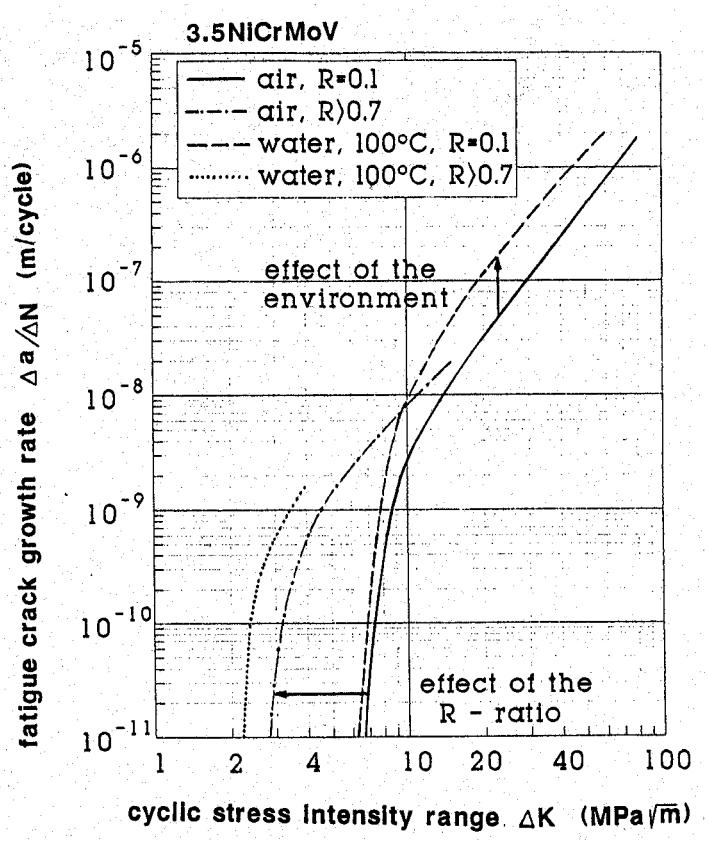

Figure 26. Corrosion fatigue crack propagation rates for disc steel (after Speidel[7,8]).

Endo et al[11] have conducted corrosion fatigue tests using a strain-controlled trapezoidal waveform with varying hold times to reflect shut down and restarting. A notched specimen was used and the results are shown in Figure 27. Clearly, hold time has a significant influence in reducing the time to crack initiation.

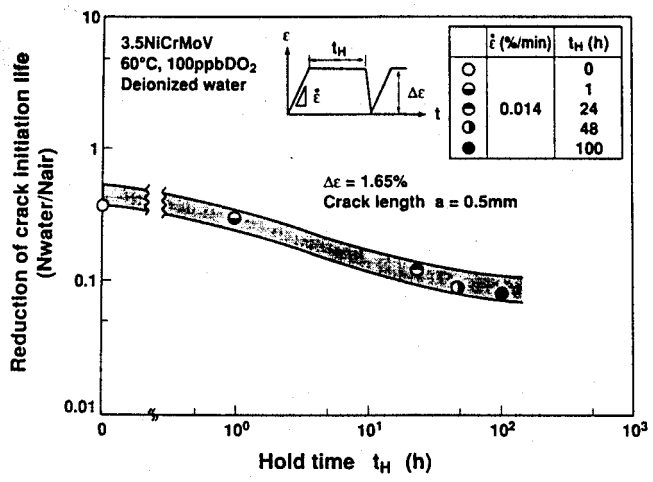

Figure 27. Impact of hold time on the number of cycles to crack initiation (after Endo et al[11]).

Using a 0.01% NaCl environment to give reasonable conductivity (compared with the basis for Figure 27) they also measured the impact of hold time on the charge passed at the notch root (sides shielded) at maximum load as shown in Figure 28. This involved conducting tests in which the current was measured in each cycle with the cycle hold time increased progressively in sequence. The electrode potential was not given and the extent to which this varied with cycle hold time not described.

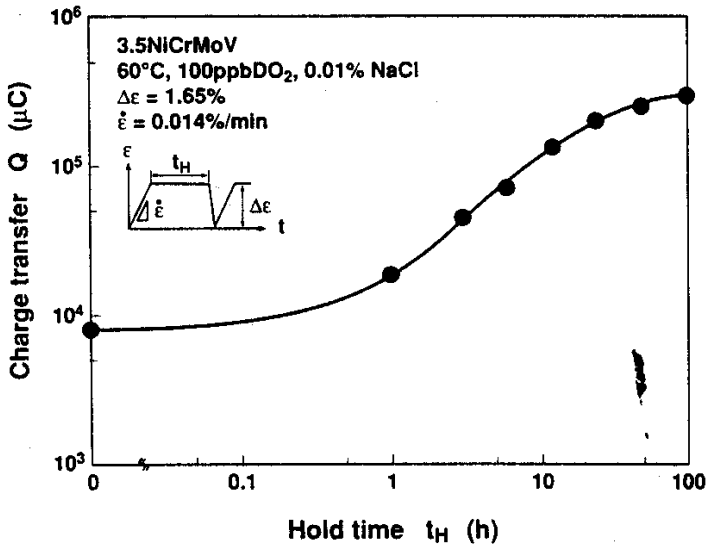

Figure 28. Measured charge passed at constant potential during corrosion fatigue testing with variable hold time (after Endo et al[11]).

Clearly, the charge passed should increase progressively with hold time since the steel is in the active state, not the passive state. The decay current is then less associated with reformation of a passive film, which if it were rapid would show an almost limiting charge at a smaller value of the hold time. In the above results the charge passed per unit time (the average current) is only slightly greater at 1 hour than 10 hours indicating that repassivation is not significant.

The issue for Figure 27 is whether the notch precluded any effect of the environment or exposure time on initiation of microcracking since the overall test time for the 100 s hold time was about 20 times that of the short hold time. Otherwise, the longer exposure time would have simply meant more opportunity for deeper pits to develop.

Recent work by Zhou and Turnbull[26] suggests a factor of 4 increase in crack growth rate compared to static loading when a trapezoidal load was used (4 hour hold and 20 mins rising and falling load) but the period of time in the loading cycle when crack extension was occurring was not clarified.

It is important to resolve the question of hold time since from the point of view of data collection this would ideally be kept as short as possible to maximise the number of test cycles. This would seem to be answered by the work of Kondo et al[20]. A notable feature was the marked effect of hold time on cycles to 'initiation' (Figure 29) but the more constrained effect on crack growth rate (Figure 30). In the latter case, increasing the hold time had little effect when the hold time exceeded a few hours.

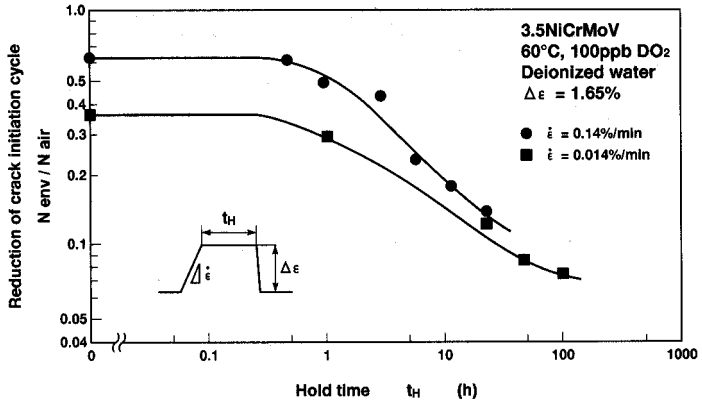

Figure 29. Impact of hold time and strain rate on the number of fatigue cycles to crack initiation (after Kondo et al[20]).

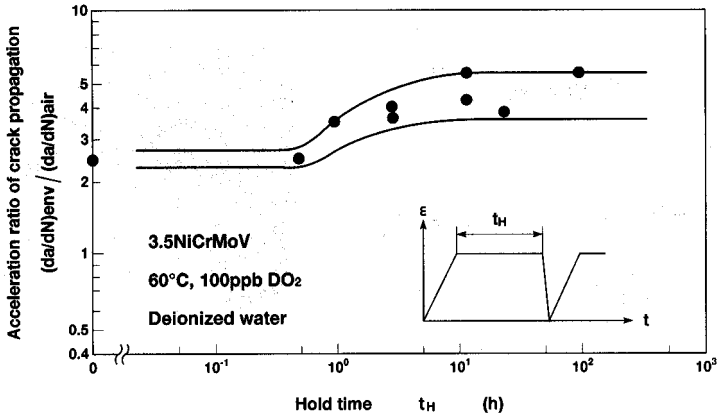

Figure 30. Impact of hold time on corrosion fatigue crack propagation kinetics(after Kondo et al[20]).

Discussion

Cracking in service

There appears a consistent strand of evidence to suggest that cracking in service is linked to ingress of oxygen in terms of correlation with air in-leakage rates and observation that oxygen can be retained for some time. As discussed in Section 1, under normal operating conditions, the oxygen concentration in the liquid film would be negligible. It is only following an off-load period, a system upset with significant air leakage, or during forced condensation that oxygen levels in the liquid film would be significant enough to influence the corrosion potential and cracking susceptibility.

In terms of the crack path, the indications are that it is predominantly intergranular but with the initial stages being transgranular. Since oxygen has been associated with transgranular cracking, the additional implication is that oxygen is likely to affect

short crack growth kinetics. The depth range over which this influence exists has not been established.

By comparison of estimated crack growth rates in service with crack growth studies in the laboratory, it can be concluded that concentrated NaOH does not have a significant effect on service behaviour. Whilst this may have some validity, the comparison cannot be extended too widely as a means of inferring service conditions since the spread in crack growth rates in the laboratory is large and the sensitivity to environmental variables is limited. It is also important to check that measurements based on cracks observed in service account for the period spent in the short crack regime.

Laboratory testing

Procedural issues

In many of the laboratory tests, the actual oxygen concentration present in the solution was not measured and the extent to which continuity of optimum conditions was maintained during the course of long laboratory tests was often not evident. In condensing steam situations, oxygen measurement would only be feasible when the steam is condensed before discharge to waste. The conductivity of the solution was also allowed to drift in some of the closed autoclave tests. Further, there are concerns that the adoption of high purity deionised water for immersion testing is not relevant to the chemistry of the liquid film, which would be expected to contain impurities at concentrations up to about 300 ppb under normal operating conditions (see Section 1).

Many of the laboratory tests were conducted using self-loaded specimens. However, for plain specimens there appeared little attention displayed in the publications to the problems in ensuring that stresses relative to yield strength *at temperature* were as defined. In some cases, retensioning was required when specimens were removed for surface crack length inspection and this can potentially impact on cracking.

It is difficult to explain the disparate results reported in relation to the observation of no pitting by David et al.[23] and by Speidel et al.[3,7,8] for immersed conditions with high quality deionised water, with the results of Gabetta and Caretta[15] clearly indicating pitting and with a more recent investigation by Zhou and Turnbull[22], in which deep pits of 100 μm were observed both in aerated and deaerated water under well controlled and maintained water chemistry. The conductivity of the deaerated solution was less than 0.1 $\mu S\ cm^{-1}$, whilst that of the aerated solution (containing dissolved CO_2 from the atmosphere) was 1 $\mu S\ cm^{-1}$. Steel quality might still be the explanation as the steel used by Zhou and Turnbull had been in service for many years, but David et al. used a 25-year old steel in their testing also.

Removal of specimens for surface crack length measurement can possibly affect the corrosion and cracking behaviour when re-immersed, depending on the exposure conditions. Some workers have taken the precaution of exposing a number of specimens in parallel systems and removing at different times to avoid this uncertainty.

In few cases, if any, were crack growth rates monitored continuously.

The spread in laboratory tests (an order of magnitude in growth rates in some cases) seems much larger than one might account for in relation to material variability. Accordingly, the significance of specific test parameters can be distinguished only if their impact on crack growth extends beyond the general variability in testing. It does not mean that there is no intrinsic effect; simply, all one can deduce is that any effect, if it does exist, is overwhelmed by other testing variables.

Strength level

There is no ambiguity about the effect of strength level when testing either plain or fracture mechanics specimens. Failure is invariably enhanced, and crack growth rates much faster with increased tensile strength.

Also, cracking of plain specimens of high strength steels when tested to yield or near yield is not related to pitting. However, there is no intrinsic material reason why pitting should not have a role in the cracking of high strength steels. It may be simply that by setting the stresses to the yield the stress values are clearly much higher in absolute terms compared with the medium strength steel. There are sound reasons for this, as the steel in service would be stressed to the higher level since that would the purpose of adopting that steel. However, it might be anticipated that pitting corrosion as an initiator of cracking may become more important if the high strength steel were tested at stress levels corresponding to that of the lower strength alloy. In practice, Holdsworth[27] has indicated that laboratory testing does not support that perspective.

Steel cleanliness

There is a little ambiguity in the test results with respect to cleanliness and crack growth rates. The work of Lyle and of Holdsworth suggests that P segregation to the grain boundary can influence the crack growth rates. The more general view is that long crack growth kinetics are unaffected by steel cleanliness for the static loading conditions tested. These apparently inconsistent results may reflect to some degree the spread in data sets.

Steel cleanliness has a big impact in reducing pitting corrosion and initiation of cracks for the medium strength steels. Pits do still initiate in the superclean steels but the pits initiate around oxide particle inclusions, the density is generally lower, and the growth rate is lower. However, the detailed study by Gabetta and Caretta[15] shows much variability although the general conclusion is valid. Nevertheless, deep pits of up to 160 μm were obtained in the superclean steel, whilst for the same exposure time of 430 h the deepest pits from the conventional steel were about 180 μm. However, once a pit has been initiated and grown beyond the initial influence of the inclusion composition in terms of pit chemistry it is not obvious why the growth rate should be faster for the conventional steel. Pit coalescence and connectivity of sulphide species in the conventional steel may explain this.

If crack initiation and development were determined by a single pit a large difference in the time for a crack to grow to a macrocrack would not be expected. Certainly, macrocracks in the superclean steel would be anticipated. There are two possibilities to explain the greater growth rate of the conventional steels: crack coalescence and

connectivity of sulphide species. The former is important when there is a high pit density, or clustering, allowing linkage of cracks initiated from different pits. Based on NPL work[22] on conventional steels such linkages are not formed in the absence of oxygen because the pit density is too low. In the work of Holdsworth et al, the condensed solution would be oxygen-free, but an impact of cleanliness is still observed. The possibility should be considered that in the early stages of crack growth a degree of connectivity of MnS inclusions is important in stimulating crack growth in the conventional steels. The rate may be variable at the local level. However, such an effect might be expected for long crack growth but is not observed.

The apparent lack of any influence of steel cleanliness on the growth rate of long cracks (leaving aside the issue of P segregation) is in contrast to the significant impact of sulphur content on the corrosion fatigue crack propagation rate of reactor pressure vessel steel. Under corrosion fatigue conditions at the lower temperatures associated with steam turbines the sulphur content of the steel might be considered a possible factor but does not appear to have been investigated. The difference between corrosion fatigue and stress corrosion cracking in this context may be the greater crack tip surface exposed during loading and the possible role of the mechanical fatigue process in bridging regions of low inclusion density.

One unresolved result is that of Lyle[16] who observed that crack initiation occurred in a shorter timescale in creviced specimens of superclean steels, relative to conventional steels. It is possible that this relates to the potential drop in the crevice, which may be greater when there is a greater density of active pits, as there would be for the conventional steel. Then, the local electrochemical driving force would be reduced. The test data refer to both 40 ppb oxygen and 6-8 ppm oxygen.

Oxygen concentration

A link between cracking in service and ingress of air suggests a key role for oxygen with the strong implication that this is related primarily to initiation. Laboratory tests in immersed condition indicate a significant impact of oxygen on pit density and growth and the density and depth of cracks.

Oxygen concentration unarguably has a key impact on pit initiation and pit growth rate. A higher potential means that the pitting potential is likely to be exceeded for a wide distribution of incipient surface sites whilst the growth rate will be enhanced also by virtue of the higher potential. However, these will depend critically on the solution conductivity and chloride concentration. A low chloride level, corresponding to near pure water for example, will give rise to a lower density of pits as the pitting potential may only be exceeded for the most active sites, whilst the growth rate will be constrained by the limitations on the effective area of external surface that can act as a supporting cathode in low conductivity solutions. In the latter case, a local potential drop will ensue that will slow the rate of growth of the pit.

Experimental evidence from refreshed water studies at NPL[22] indicates clearly that pit growth kinetics and density are much higher in air-saturated 1.5 ppm chloride solution when compared with air-saturated or deaerated pure water. For example, the maximum depths were about 3 times greater.

In stress corrosion cracking tests at 90 °C, tensile specimens loaded to 90% of the 0.2% proof stress showed abundant cracks with indication of coalescence in the chloride-containing solution but no cracks at all in the air-saturated chloride–free solution even with pit depths of nearly 200 μm. Since cracks were observed to initiate from similar size pits in the chloride-containing solution, the absence of cracking in the pure water is most likely due to the lower potential in the pit base in that case. These observations are consistent with the results shown in Figure 17.

The incidence of pitting will also depend on the test conditions. For example, a stagnant aerated solution under autoclave conditions may develop an enhanced conductivity local to the sites of corrosion due to dissolution of inclusions and poor mixing. Later, contamination of the bulk solution from corrosion products may ensue.

In general terms, oxygen may enhance the susceptibility to cracking irrespective of whether it has any *direct* impact on the growth rate simply by virtue of encouraging pit density and growth. The more challenging question to answer from the data available is the extent to which oxygen impacts directly on the very early stages of crack growth, and under what circumstances does it influence long crack growth kinetics.

In the context of high strength steels, which are not so affected by the issue of pitting and correspondingly perhaps not crack coalescence since the stresses are high enough (when tested close to yield), there is evidence that oxygen has an impact on cracking of plain specimens as shown by Figure 17. Thus, it would appear that oxygen does have an important effect even though pits are considered not to be the site for crack initiation. More likely, localised slip at the high stresses concentrated at microstructural features may be sufficient, with oxygen affecting the local dissolution kinetics. However, since the mechanism of cracking is presumed to be hydrogen embrittlement the effect of oxygen has to be explained as this makes the potential more noble and less conducive to hydrogen uptake. It may be the case that microscopic defects at grain boundaries or other initiation site are created by local dissolution within which some local changes in solution chemistry encourages hydrogen uptake.

The one important piece of work that appears to conflict with the ideas above is that of Holdsworth and colleagues[19] using condensing steam with different oxygen levels in the feedwater. To some extent an explanation can be found in the deduction that a condensed layer in pure condensing steam (not air-contaminated) contains negligible oxygen irrespective of the oxygen concentration in the feed water. This would reconcile some of the observations but the lack of response under two-shifting conditions in which there was air ingress is not readily explained. Also, if that system were wholly oxygen-free, the growth rate is surprising, although continued exposure tests at NPL in oxygen-free solution might help to clarify the position.

Clearly, when oxygen is present in the solution a significant increase in the corrosion potential occurs to more positive values with the extent being dependent on chloride level. The solution in a long crack is wholly oxygen-free and if uncoupled to the external surface would adopt a potential associated with deaerated water, i.e. about -0.700 V SCE (-440 V SHE) or so. The issue then is the extent to which the crack-tip and external surface remote from the crack are coupled through the solution. In pure

water, with the conductivity so low, such coupling would be expected to be ineffective and the crack tip conditions, and hence crack growth, will not be affected by aeration of the bulk solution. This is wholly compatible with a number of the experimental observations on long crack growth kinetics; i.e. there is no effect of oxygen.

As the bulk solution conductivity increases, the possibility of coupling between the crack tip and bulk solution increases but will be influenced by crack depth. There are no experimental data to establish the critical bulk solution conductivity at which an impact of oxygen might be expected. Theoretical modelling suggests a possible impact around 2 $\mu S\ cm^{-1}$. However, Kondo noted that with nominally 100 ppb oxygen at 60 °C, crack propagation rates were unaffected by increasing the conductivity to almost 30 $\mu S\ cm^{-1}$, whilst crack initiation was affected. It is possible that the corrosion potential was not high, similar to the low end of the curve in Figure 12 (albeit at 160 °C here).

The one study that conflicts with the view that the oxygen concentration of the bulk solution has no impact on crack growth rates is the work of McMinn et al who reported a marked increase in growth rates of WOL cracks when using aerated pure water compared with deaerated pure water (Figure 20). Cracking was transgranular, as noted also for the CERT tests reported in Figure 12.

There is no mechanistic framework that can readily account for these disparate results. It emphasises that the corrosion potential should be monitored wherever possible so that confidence in the data can be generated.

In relation to service conditions, the turbine discs are exposed to aerated solutions off-load and the system should be oxygen free whilst on-load. The chloride level in the condensate off-load will be very small, a few ppb, whilst on-load it could be around 300 ppb and possibly as much as 1.5 ppm. The rate at which film formed off-load breaks down when the oxygen concentration is reduced is not known but conceivably a transient high potential with chloride present is feasible. Cycling of the environment during laboratory testing would be informative.

Carbon dioxide

Although no apparent effect of CO_2 on long crack growth kinetics is reported[3,7,8], there is an exception in the work of McMinn et al. It is surprising that no effect was observed by Speidel et al despite testing with 100 ppm CO_2 (Figure 19), since a pH of about 4.5 would be predicted and the conductivity could be significant. In long cracks, the change in pH of the bulk solution will have no *direct* impact on crack chemistry. However, it might have been expected that a somewhat higher potential (due to the reduction of hydrogen ions at the lower pH) combined with the increased conductivity would have allowed more crack-tip polarisation. Further investigation is warranted to rationalise these results.

In relation to testing of plain specimens, there appears to be no systematic study of the effect of CO_2 concentration on stress corrosion cracking resistance. There is some indication of a significant increase in propensity for crack initiation in CO_2-containing environments in the work of Schleithoff, but the specific values of CO_2

used in these full immersion tests need clarified and in particular the relevance to the CO_2 level expected in liquid films under normal operational conditions, which is expected to be of the order of 1 ppb (see Section1).

Two-shifting

The data of Holdsworth et al from testing of plain specimens suggest that cycling the environment has little impact on microcrack development compared with tests in sustained steam condensing conditions.

However, there is clear evidence from the work of Kondo et al that cycling the load to simulate two-shifting does accelerate initiation and crack growth rates. In the latter case, an effect of hold time would not seem to prevail beyond a few hours. Zhou and Turnbull[26] also observed a significant effect of load cycling on crack growth rate.

Crevice specimens

The rationale behind the use of crevice specimens is that these represent the keyway region for example but in more general use creviced specimens are designed to create differential aeration cells. The initial puzzle of the work of Lyle et al. is that creviced specimens are quite susceptible to cracking even in deaerated solutions. The most obvious explanation would be that the crevice helps to retain the products of MnS dissolution thereby making crack initiation and propagation more likely. There will be a balance between generating local concentrations of aggressive species and minimising potential drop, which could arise if there is too much corrosion activity.

Conclusions

- Pitting appears to occur more readily in oxygen-containing solutions.

- The consensus is that there is no effect of oxygen on the growth of long cracks in pure water outwith the general spread of data. However, the results of McMinn et al, showing a factor of ten increase in growth rate for aerated pure water compared with deaerated pure water, represent a possible exception

- There is too limited a range of data to establish the critical combination of oxygen concentration and chloride concentration (or more generally solution conductivity) at which long crack propagation would be affected.

- Like oxygen, CO_2 appears to enhance crack initiation but to have little influence on long crack propagation rates. However, in the latter case, there is no unanimity of data and further work is required.

- Measurement of crack tip potential for different combinations of chloride and oxygen and/or CO_2 would give insight in resolving these issues.

- The significance of both oxygen and CO_2 is greater the higher the strength level, despite the limited influence of pitting for this case.

- The extent to which short crack growth kinetics are affected by oxygen or CO_2 has not been established. However, in terms of the crack path in service, the indications are that it is predominantly intergranular but with the initial stages being transgranular. Since oxygen has been associated with transgranular cracking, the additional implication is that oxygen is likely to affect short crack growth kinetics. The depth range over which this influence may exist is not established.

- Steel cleanliness reduces the incidence of pitting and crack initiation of medium strength steels but its effect on long crack propagation does not appear generally significant. However, two sets of results suggest some impact on crack growth rate of P at the grain boundaries.

- For high strength steels, steel cleanliness is considered not to have an impact on initiation but this may reflect simply the higher stresses when testing as a percentage of yield.

- Two-shifting increases the crack growth rate with respect to the load changes. However, the impact of cycling the atmosphere exposure conditions would seem modest in condensing steam conditions. Nevertheless, further work is required.

- Testing the impact of coupling of the 12 Cr steel with the 3.5 NiCrMoV steel in a crevice arrangement would be of value because of the possible low pH in the crevice expected for the 12 Cr steel.

Acknowledgements

This work was conducted as part of the "Life Performance of Materials" programme, a joint venture between the United Kingdom Department of Trade and Industry and an Industrial Group comprising Alstom, BNFL Magnox, British Energy, Innogy, Powergen and Siemens. The authors are grateful to the members of this Industrial Group for their support and advice and to T. B. Gibbons for his critical review of the manuscript.

References

1. A. McMinn, F.F. Lyle Jr., and G.R. Leverant, Corrosion, Vol.41, No 9, 1985 and also Proc. Inst. Mech. Engrs., Vol 199, No A1, 1985, 59-67.
2. N. Sastry Cheruvu and B.B. Seth, PWR-Vol 21, 'The steam generator today: materials, flow path design, repair and refurbishment', ASME 1993, quoting X. Baldino et al, Proc. American Power Conf. Vol 45, 1983, 184.
3. M. Speidel and R. Magdowski, 'Stress corrosion cracking of steam turbine steels – An overview', 2nd Int. Symp. Environmental Effects on Degradation in Nuclear Power Plants, Monterey, 9-12 Sept, 1985, pp 267-275.
4. J.M. Lyons and J. Corish, Corros. Sci., Vol. 38, No 8, 1331-1356, 1996.
5. D.A. Rosario, R. Viswanathan, C.H. Wells and G.J. Licina, Corrosion, Vol. 54, No 7, 531, 1998.
6. J. Denk, 'Low pressure steam turbine integrity', Proc. Materials for Advanced Power Engineering, Liege, Belgium, 3-6 Oct, 1994, pp 157-170.

7. M.O. Speidel, J. Denk, and B. Scarlin, 'Stress corrosion cracking and corrosion fatigue of steam-turbine rotor and blade materials', Cost Project, EUR 13186 EN, 1991.
8. M.O. Speidel and B. Scarlin, 'Stress corrosion cracking and corrosion fatigue of steam-turbine rotor and blade materials', Proc. High Temperature Materials for Power Engineering, Liege, Belgium, 24-27 Sept, 1990, pp 343-368.
9. R. Viswanathan, 'Clean/Superclean steel rotors for electric utility applications', Steel Forgings: Second volume, ASTM STP 1259, Eds E.G. Nisbett and A.S. Melilli, ASTM, 1997, pp 280-303.
10. S.R. Holdsworth and G. Burnell, 'Stress corrosion cracking of LP steam turbine rotor steels', GEC Report RM852/88, January 1989.
11. T. Endo, H. Itoh, Y. Kondo, H. Karato, 'Material aspects for the prevention of environmentally-assisted cracking in low pressure steam turbine', PWR-Vol 21, The Steam Turbine Generator Today: Materials, Flow Path Design, Repair and Refurbishment, ASME 1993, pp 75-82.
12. P. McIntyre, P. Mulvihill and P.J. Trant, CEGB Report RD/L/FWC/0016/M89, 1988.
13. S.R. Holdsworth and D.V. Thornton, 'Resistance of superclean 3.5 NiCrMoV steels to stress corrosion cracking in pure steam', Proc. of the Robert I. Jaffe Memorial Symposium on Clean Materials Technology, ASM Materials Week, Chicago, Illinois, 2-5 Sept. 1992, pp 197-204.
14. S. R. Holdsworth, M. Nougaret and B. Vittemant, 'Stress corrosion in 3.5 NiCrMoV welded joints, Proc. Conf Clean Steel: Superclean steel', March 6-7, 1995, IOM, London, 1996.
15. G. Gabetta and E. Caretta, 'Investigation on pit susceptibility in low pressure rotor steels', Proc. Materials for Advanced Power Engineering, 1994, 3-6 Oct, Kluwer Academic Press, Dordrecht, pp 209-218.
16. F.F. Lyle, Jr., 'Stress corrosion crack initiation in low-pressure steam turbine disc steels', 6th Int. Symp. on Environmental Degradation of Materials in Nuclear Power Systems-Water Reactors, Eds R.E. Gold and E.P. Simonen, The Minerals Metals and Materials Society, 1993, 121- 128.
17. W.G. Clark Jr., B.B. Seth and D.H. Shaffer, 'Procedures for estimating the probability of steam turbine disc rupture from stress corrosion cracking', ASME paper at ASME/IEEE Power Generation Conference, October 1981.
18. A.McMinn, F.F. Lyle and G.R. Leverant, J. Materials for Energy Systems. Vol. 6, No. 3, 1984, pp. 184-199.
19. S.R. Holdsworth, M. Nougaret, B.W. Roberts and D.V. Thornton, 'Laboratory stress corrosion cracking experience in steam disc steel' (unpublished report), GEC Alstom.
20. Y. Kondo, M. Bodai, M. Takei, Y. Sugita and Inagaki, in Effects of environment on the initiation of crack growth, eds W. A. van der Sluys, R. S. Piascik and R. Zawierucha, ASTM STP 1298, 1997, pp 120-134.
21. K. Schleithoff, 'Influence of water steam chemistry on stress corrosion cracking of steam turbine LP discs', Corrosion in Power Generating Equipment, eds M.O Speidel and A. Atrens, 1984, Plenum Press, New York, pp 361-365.
22. S. Zhou and A. Turnbull, NPL, work in progress.
23. W. David, G. Rottger, K. Schleithoff, H. Hamel and H. Termuehlen, 'Disk-type LP turbine rotor experience', PWR-Vol 21, The Steam Turbine Generator Today: Material, Flow Path Design, Repair and Refurbishment, ASME 1993, pp 83-91.

24. G.M. Sparkes, P. Mulvihill and P. McIntyre, ‘The implications of corrosion pitting for the refurbishment of low-pressure turbine rotor shafts’, Proc. Refurbishment and Life Extension of Steam Plant, 14-15 Oct, London, I. Mech. E, 1987.
25. J.M. Hodge and I.L. Mogford, Proc.: I. Mech. E. Vol. 193, No. 11, 93, 1979.
26. S. Zhou and A. Turnbull, ‘Environment assisted cracking of steam turbine disc and blade steels - description of test procedure and preliminary results’, NPL Report, MATC(A)41, 2001.
27. S Holdsworth, Alstom, Private Communication, 2002.